Front. Optoelectron. 2014, 7(3): 300–319
DOI 10.1007/s12200-014-0435-1

REVIEW ARTICLE

Silicon hybrid nanoplasmonics for ultra-dense photonic integration

Xiaowei GUAN, Hao WU, Daoxin DAI (✉)

State Key Laboratory for Modern Optical Instrumentation, Centre for Optical and Electromagnetic Research, Zhejiang Provincial Key Laboratory for Sensing Technologies, Zhejiang University, Hangzhou 310058, China

Abstract Recently hybrid plasmonic waveguides have been becoming very attractive as a promising candidate to realize next-generation ultra-dense photonic integrated circuits because of the ability to achieve nano-scale confinement of light and relatively long propagation distance. Furthermore, hybrid plasmonic waveguides also offer a platform to merge photonics and electronics so that one can realize ultra-small optoelectronic integrated circuits (OEICs) for high-speed signal generation, processing as well as detection. In this paper, we gave a review for the progresses on various hybrid plasmonic waveguides as well as ultrasmall functionality devices developed recently.

Keywords plasmonics, hybrid, silicon, nanowire, integration

1 Introduction

To achieve photonic circuits with ultra-high integration density, it has been desired for a long time to have nano-scale optical waveguides with strong confinement of light. Three kinds of typical nanophotonic waveguides have been developed in the past years, which includes nanophotonic wires (strip nano-waveguide) [1,2], photonic-crystal waveguides [3] and nanoplasmonic waveguide [4–16]. The former two nanophotonic waveguides, which utilize nano-structures with ultra-high index contrast, cannot be beyond the diffraction limit. In contrast, a nanoplasmonic waveguide can break the diffraction limit and enable deep subwavelength confinement and waveguiding of light, which makes it become a very attractive candidate for ultra-high integration density. A nanoplasmonic waveguide also offers a way to merge electronics and photonics [17] so that it is potential to realize ultra-small optoelectronic integrated circuits (OEICs) for low power-consumption and high speed signal generation, processing as well as detection. Several years ago, some nanoplasmonic waveguides supporting ultra-highly localized fields were proposed and demonstrated, including metal nano-slot waveguides [8–10,15,16] and metal V-groove waveguides [11,12]. However, these nanoplasmonic waveguides have large losses and their propagation distance is very limited (usually ~μm).

More recently hybrid plasmonic waveguides [18–21], which consist of a high-index region, a metal region and a low-index nano-slot between them, have been paid intensive attention to Refs. [22–43] It has been shown that hybrid plasmonic waveguides have the potential to achieve a nano-scale light confinement as well as relatively long propagation distance simultaneously. In 2007, Alam et al. proposed the initial form of a hybrid plasmonic waveguide including a lossy dielectric nanowire adjacent to a metal surface [18]. It was shown that a super-mode exists due to the coupling between a surface-plasmonic mode and a dielectric-waveguide mode. The mode properties of this super-mode were investigated in the wavelength range from 0.5 to 1.2 μm (which is not the transparent window of silicon and out of the telecommunication window) and the calculated full width at half maximum (FWHM) of the demonstrated supermode is about 400 nm (~$\lambda/3$ when operating at 1.2 μm), which is not as small as that achieved by those hybrid nanoplasmonic waveguide proposed later [19–21]. In Ref. [19], the name of hybrid plasmonic waveguide was proposed formally and a hybrid plasmonic waveguide operating at 1550 nm was obtained by putting a dielectric cylinder above a metal surface, for which the mode area was as small as $\lambda^2/400$. With this kind of hybrid plasmonic waveguide, a nano-laser emitting 489 nm light was

Received April 16, 2014; accepted June 13, 2014

E-mail: dxdai@zju.edu.cn

demonstrated in 2009 [43]. In comparison with the hybrid plasmonic waveguide with a cylinder, a nano-waveguide with a rectangular cross section would be more useful from a view point of fabrication and integration [20,21]. In Ref. [20], the authors has given an analyses for the dispersion relation and loss of the modes in several types of metal-GaAs nanoplasmonic waveguides, including a rectangular GaAs strip above Ag-substrate (which is very similar to that shown in Refs. [18,19]), and a lateral GaAs-gap-Ag strip on a SiO_2 substrate (which is not easy to fabricate). For these early hybrid plasmonic waveguides [18,19], the surface plasmonic effect occurs at the top-surface of the metal thin film and unfortunately the metal top-surface is usually quite rough, which would introduce some notable scattering loss.

As it well known, silicon photonics have become very popular because of the compatibility with mature complementary metal oxide semiconductor (CMOS) technologies with low cost and excellent processing control. And silicon-on-insulator (SOI) nanowires are usually used for silicon nanophotonic integrated circuits. Therefore, it would be attractive to develop a silicon hybrid nanoplasmonic waveguide which is SOI-compatible so that it can be fabricated on a standard SOI wafer by using CMOS-compatible processes. In our previous paper, we have presented a SOI nanowire with a metal cap which is used for a submicron-heater [22], and there is a low-index region (e.g., SiO_2) between the silicon core and the metal cap. When the SiO_2 layer becomes very thin (e.g., several tens of nanometers), a silicon hybrid nanoplasmonic waveguide (with a metal cap) is achieved, as proposed first in Ref. [21]. This silicon hybrid nanoplasmonic waveguide has a field enhancement at the thin low-index region for the hybrid plasmonic mode (transverse magnetic (TM) polarization) and the spot size can be as small as 50 nm $\times$ 5 nm when operating at 1550 nm. Particularly, for this silicon hybrid nanoplasmonic waveguide, the surface plasmonic effect occurs at the metal bottom-surface, which is as smooth as the top surface of the low-index thin film. This is important and helpful to obtain low scattering loss of surface. This might make it more attractive than those hybrid plasmonic waveguide on a metal surface. Furthermore, the SOI-compatibility of the proposed silicon hybrid nanoplasmonic waveguide makes the fabrication simplified, and it becomes feasible to integrate a nanoplasmonic circuits and a silicon nanophotonic circuit on the same chip conveniently. Therefore, the silicon hybrid nanoplasmonic waveguide has been attracting lots of attention and various hybrid nanoplasmonic waveguides with some modifications have been proposed in the following years [44–65]. Silicon hybrid nanoplasmonic waveguide for transverse electric (TE) polarization can also be obtained by e.g., introducing double low-index vertical nano-slots at both sides of a high-index region [49–55]. In Section 2.2, various hybrid nanoplasmonic waveguides will be reviewed and compared.

With these proposed hybrid plasmonic waveguides, some ultracompact functionality elements have been realized, including directional couplers [59–63], power splitters [64–68] and grating reflectors [69]. Since the hybrid plasmonic waveguide enables a submicron bending radius [53,64,70,71], one can realize ultra-compact resonators, including submicron rings/donuts [65,66,71–75], disks [76,77] and photonic-crystal cavities [78–80], as the well-known versatile elements in photonic integrated circuits. Such resonators have ultra-compact footprint as well as good performances (e.g., acceptable quality factor and large Purcell efficiency [77]). Furthermore, as it well known, hybrid plasmonic waveguides are very polarization-sensitive, which is helpful for realizing ultrasmall polarization-handling devices, including polarizers [81–86], polarization-beam splitters (PBS) [87–92], and polarization rotators [93–95]. These will be also reviewed in Section 3.4.

Regarding that a hybrid plasmonic waveguide is still not a good option for long-distance (e.g., 10^3-10^4μm) optical interconnects if there is no assistance from gain mediums [50], it might be a promising way to combine a silicon hybrid nanoplamonic waveguide and a low-loss SOI nanowire [72]. This way, the low-loss SOI nanowire enables a long-distance optical interconnect while the hybrid nanoplamonic waveguide is used locally to realize some functionality elements with ultrasmall footprints. To realize the seamless integration between hybrid plasmonic circuits and silicon nanophotonic circuits, two coupling approaches can be utilized. One is the evanescent coupling structure designed according to the phase-matching condition [63] and the other is the butt-coupling structure (which provides an efficiency of 70%–80% with a very short mode converter [96]).

To compensate the intrinsic loss of hybrid plasmonic waveguides, a general way is to introduce some gain medium, in which way active hybrid plasmonic devices can be also realized. For example, a deep subwavelength plasmonic laser has been demonstrated experimentally, by using a hybrid plasmonic waveguide with a CdS cylinder above a silver plate [43]. For silicon hybrid plasmonics, the nano-slot can be filled in with some low-index gain medium, e.g., Er-doping, quantum dots, Si nano-crystals, etc. Due to the field enhancement in the low-index nano-slot region, some gain enhancement is observed [47]. In Section 4.1, we will give a discussion on the loss issue of silicon hybrid nanoplamonic waveguide. Furthermore, the field enhancement in the nano-slot also makes the hybrid plasmonic waveguide very promising for the applications including highly-efficient optical modulation [97–102], nonlinear optical effects (like optical parametric amplifier [103]), optical sensing with high sensitivity [104–106], and enhanced optical forces [107,108]. This will be summarized in Section 4.2.

2 Silicon hybrid nanoplasmonic waveguides

2.1 Principle of silicon hybrid nanoplasmonic waveguides

To understand the guided-mode mechanism for a hybrid nanoplasmonic waveguide (which usually consists of a high refractive-index (RI) region, a metal layer and a low-RI region between them), first we consider a hybrid slab waveguide with the same layer structure for which the analytical expressions for the eigen-modes can be obtained. The hybrid slab waveguide has a low-index cladding, a high-index layer, a low-index layer and the metal layer, as shown in Fig. 1(a). According to Maxwell's equation, the electric field distribution of the TM fundamental mode for the slab waveguide is given as

$$E_y = \frac{1}{n_{\mathrm{M}}^2} A_{\mathrm{M}} \exp\left(-\gamma_{\mathrm{M}}(y - t_{\mathrm{L}})\right), t_{\mathrm{L}} < y < +\infty, \quad (1)$$

$$E_y = \frac{1}{n_{\mathrm{L}}^2}[A_{\mathrm{L1}} \exp\left(\gamma_{\mathrm{L}}(y - t_{\mathrm{L}})\right) + A_{\mathrm{L2}} \exp(-\gamma_{\mathrm{L}} y)], 0 < y < t_{\mathrm{L}}, \quad (2)$$

$$E_y = \frac{1}{n_{\mathrm{L}}^2} A_{\mathrm{H}} \cos(k_{\mathrm{H}} y - \varphi), -t_{\mathrm{H}} < y < 0, \quad (3)$$

$$E_y = \frac{1}{n_{\mathrm{S}}^2} A_{\mathrm{S}} \exp\left(\gamma_{\mathrm{S}}(y + t_{\mathrm{H}})\right), y < -t_{\mathrm{H}}, \quad (4)$$

where the constants A_{M}, A_{L1}, A_{L2}, A_{H} and A_{S} are determined according to the boundary conditions at the corresponding interfaces between adjacent layers. And the complex propagation constant can be achieved by solving the following eigen-equations

$$k_{\mathrm{H}} t_{\mathrm{L}} = n\pi + \tan^{-1}\left(\frac{\gamma_{\mathrm{S}} n_{\mathrm{H}}^2}{k_{\mathrm{H}} n_{\mathrm{S}}^2}\right) - \tan^{-1}\left(\frac{\gamma_{\mathrm{L}} n_{\mathrm{H}}^2}{k_{\mathrm{H}} n_{\mathrm{L}}^2} \frac{1 - \frac{\gamma_{\mathrm{L}} n_{\mathrm{M}}^2 + \gamma_{\mathrm{M}} n_{\mathrm{L}}^2}{\gamma_{\mathrm{L}} n_{\mathrm{M}}^2 - \gamma_{\mathrm{M}} n_{\mathrm{L}}^2} \exp(2\gamma_{\mathrm{L}} t_{\mathrm{H}})}{1 + \frac{\gamma_{\mathrm{L}} n_{\mathrm{M}}^2 + \gamma_{\mathrm{M}} n_{\mathrm{L}}^2}{\gamma_{\mathrm{L}} n_{\mathrm{M}}^2 - \gamma_{\mathrm{M}} n_{\mathrm{L}}^2} \exp(2\gamma_{\mathrm{L}} t_{\mathrm{H}})}\right), \quad (5)$$

where, n_{M}, n_{L}, n_{H}, and n_{S} are the indices for metal, the low-index layer, the high-index layer, and the substrate, respectively,

$$k_0^2 n_{\mathrm{H}}^2 - k_{\mathrm{H}}^2 = k_0^2 n_{\mathrm{M}}^2 + \gamma_{\mathrm{M}}^2 = k_0^2 n_{\mathrm{L}}^2 + \gamma_{\mathrm{L}}^2 = k_0^2 n_{\mathrm{S}}^2 + \gamma_{\mathrm{S}}^2 = \beta^2,$$

in which k_0 is the wavenumber of the light in vacuum.

Figures 1(b)–1(d) show the profiles for the electric field E_y of the fundamental mode in the hybrid slab waveguide as the low-index-layer thickness t_{L} decreases. As mentioned in the introduction, it is promising to choose SOI wafers for the hybrid plasmonic structure. Therefore, in this example Si and SiO_2 are chosen as the materials for the high-index layer and the low-index layer, respectively. The wavelength λ = 1550 nm and the corresponding refractive indices for all the involved materials as n_{metal} = 0.1453 + 11.3587i (Ag) [19], $n_{\mathrm{SiO_2}}$ = 1.445, and n_{Si} = 3.455. The thickness of the silicon layer is assumed to be 220 nm. One should realize there are two eigen modes in such a hybrid slab waveguide. One is the dielectric mode confined well in the Si region and the other one is the surface plasmonics mode at the interface between SiO_2-metal.

When the thickness of the low-index (e.g., SiO_2) layer between Si and metal is large (e.g., 0.5 μm), these two eigen modes are little overlapped and the dielectric mode confined in the silicon region is influenced by metal very slightly, as shown in Fig. 1(b). In this case, the dielectric mode is used usually for the photonic integrated circuits, which is the case of using metal heater for thermal tuning. One should note that there are field enhancements at the top and bottom surfaces of the SiO_2 layer. The field enhancement at the Si-SiO_2 interface is due to a strong discontinuity of the normal component of the electric field, which is the same as that in a pure-dielectric horizontal slot waveguide [2]. On the other hand, at the SiO_2-metal interface, surface-plasmonic wave is excited. The electric field of the excited surface-plasmonic wave decays exponentially at both sides of the interface and has a peak at the interface. As shown in Eq. (2), the field distribution in the thin SiO_2 layer ($0 < y < t_{\mathrm{L}}$) is as the sum of two exponential functions. Therefore, when the SiO_2 thickness becomes less than the penetration depth of the evanescent wave (e.g., < 100 nm), the dielectric mode and the surface plasmonic mode become overlapped and coupled. And there is a field enhancement in the low-index layer, as shown in Fig. 1(d) and the mode is confined tightly in the low-index region.

2.2 Structures of silicon hybrid nanoplasmonic waveguides

Similarly, a silicon hybrid nanoplasmonic waveguide shown in Fig. 2(a) has a significant field enhancement in the low index region, as shown by the curve of $E_y(0, y)$ in Fig. 2(b). In this example, the wavelength λ = 1550 nm and the geometrical dimensions are chosen as follows: w_{co} = 200 nm, h_{m} = 100 nm, h_{slot} = 50 nm, and $h_{\mathrm{rib}} = H$ = 300 nm. In Ref. [21], it has shown that a silicon hybrid nanoplasmonic waveguide has a spot-size as small as 50 nm × 5 nm even when operating at 1550 nm and the propagation distance is as long as several tens of microns. It can be seen that a hybrid plasmonic waveguide provide a promising platform to realize ultra-dense photonic integration. In the past years (from 2009 to 2014), people have developed various hybrid plasmonic waveguides

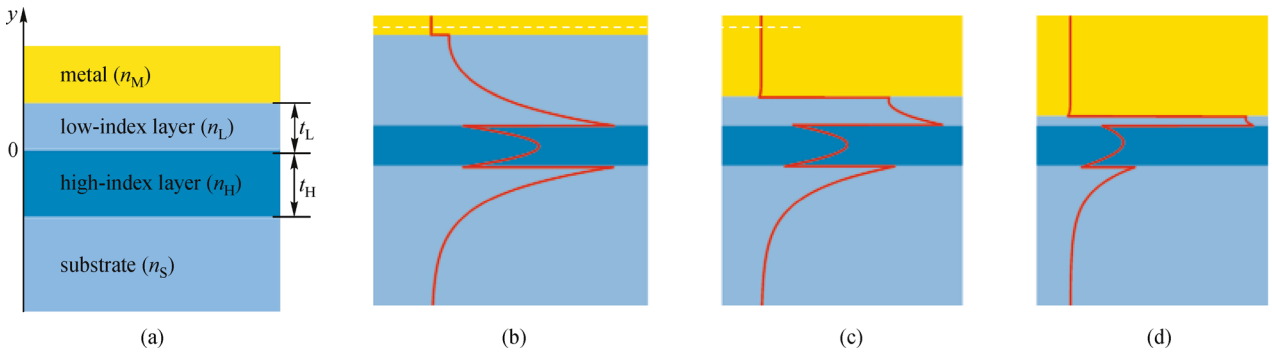

Fig. 1 (a) Configuration for a hybrid slab waveguide; the electric field E_y in a hybrid slab waveguide when (b) t_L = 500 nm; (c) t_L = 150 nm; (d) t_L = 50 nm

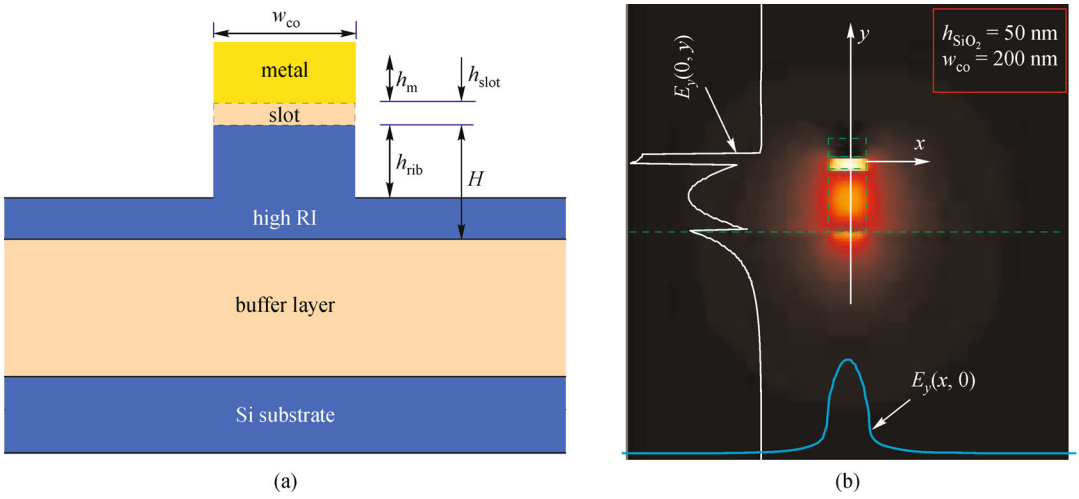

Fig. 2 (a) Cross section of a hybrid plasmonic waveguide with a metal cap; (b) calculated field distribution for the major component $E_y(x,y)$ of the quasi-TM fundamental mode of the hybrid plasmonic waveguide with w_{co} = 200 nm and h_{slot} = 50 nm. In this figure, the field distributions $E_y(0, y)$ and $E_y(x, 0)$ are also shown [21]

[24 – 42,44 – 58]. In principle, a hybrid plasmonic waveguide can be formed with e.g., a cylindrical wire [19] or a rectangular cross section [20]. The cylindrical one is pretty successful when it was proposed first in 2008 [19] and a hybrid plasmonic waveguide with a silicon cylinder were also demonstrated later [26,27]. On the other hand, a nanowaveguide with a rectangular cross section would be more useful than a cylindrical hybrid plasmonic waveguide regarding the fabrication and integration [21]. Therefore, here we focus on the silicon hybrid nanoplasmonic waveguides with rectangular structures as summarized in Table 1.

As shown in Table 1, in 2007 Alam et al. proposed the initial form of a hybrid plasmonic waveguide including a lossy dielectric nanowire adjacent to a metal surface [18] and the calculated FWHM of the supported supermode is about 400 nm (~λ/3 when operating at 1.2 μm), which is much larger than that achieved by those hybrid nanoplasmonic waveguide proposed in the following years [44–55]. Note that the surface plasmonic effect in this hybrid plasmonic waveguide occurs at the top-surface of the metal thin film and unfortunately the metal top-surface is usually quite rough. The roughness for the top surface of the sputtered silver thin film is ~20 nm (see the scanning electron microscope (SEM) picture for a sputtering silver surface shown in Fig. 3). This will introduce some notable scattering loss. Furthermore, for such a hybrid plasmonic waveguide with the metal thin film at the bottom, a standard SOI wafer is not available and one usually needs to deposit amorphous silicon thin film [40]. In 2009, a silicon hybrid nanoplasmonic waveguide with a metal cap is proposed first [21]. For this waveguide, the silicon ridge can be even modified to be a silicon slab so that the fabrication can be simplified further. The spot-size is as small as 50 nm × 5 nm when operating at 1550 nm and the calculated propagation loss is ~0.1 dB/μm. The surface plasmonic effect in this silicon hybrid nanoplasmonic waveguide occurs at the metal bottom-surface, which is as smooth as the top surface of the low-index thin film to help obtain low scattering loss of surface. More importantly, a

Table 1 Reported silicon hybrid nanoplasmonic waveguides with rectangular structures

Ref.	year	configuration	theory/ experiment	features
[18]	2007	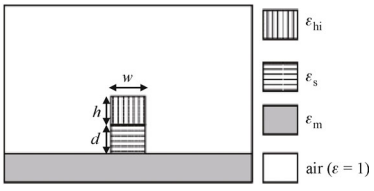	theory	structure: Si-SiO_2-Ag λ: 500–1200 nm FWHM: 400 nm L_{prop}: 13.5 μm
[21]	2009	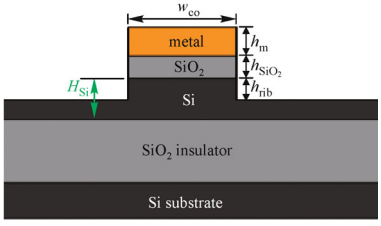	theory	structure: Ag-SiO_2-Si λ: 1550 nm W_{WG}: 50 nm L_{prop}: 90 μm
[45]	2010	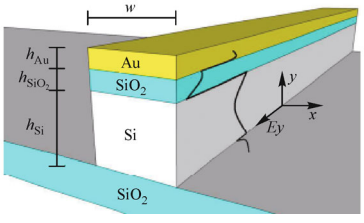	experiment	structure: Au-SiO_2-Si λ: 1550 nm W_{WG}: 250 nm L_{prop}: 40 μm
[49]	2010	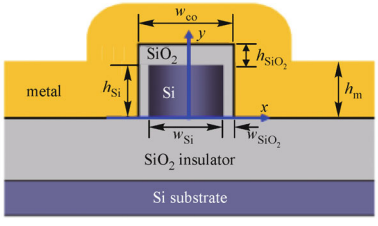	theory	structure: Ag-SiO_2-Si-SiO_2-Ag λ: 1550 nm Si-core width: 50 nm A_{eff}: 0.007 μm^2 L_{prop}: ~20 μm
[47]	2011	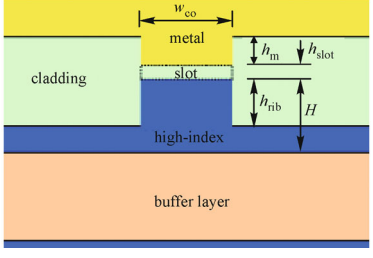	theory	structure: Ag-SiO_2-Si λ: 1550 nm W_{WG}: 70 nm loss: ~0.1 dB/μm A_{eff}: 0.066 μm^2
[51]	2011	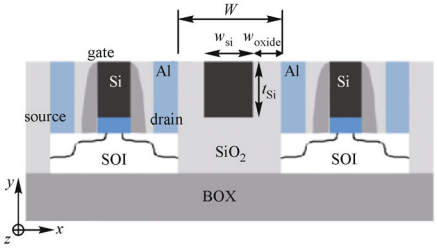	theory	structure: Al-SiO_2-Si-SiO_2-Al λ: 1550 nm Si-core width: 300 nm L_{prop}: ~31 μm

(*Continued*)

Ref.	year	configuration	theory/ experiment	features
[53]	2011	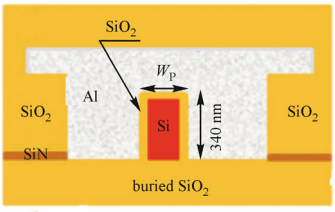	experiment	structure: Al-SiO_2-Si-SiO_2-Al λ: 1550 nm Si-core width: 43 – 136 nm loss: 1.07 – 1.63 dB/μm
[54]	2011	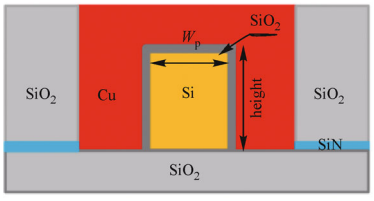	experiment	structure: Cu-SiO_2-Si-SiO_2-Cu λ: 1550 nm Si-core width: 21 – 134 nm loss: 0.37 – 0.63 dB/μm
[55]	2011	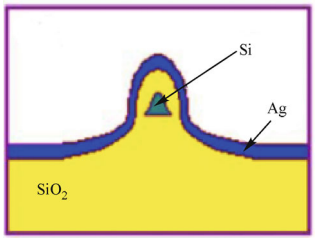	experiment	structure: Ag-SiO_2-Si-SiO_2- Ag λ: 1550 nm Si-core width: 300 nm; propagation loss: 1.6 dB/mm
[65]	2012	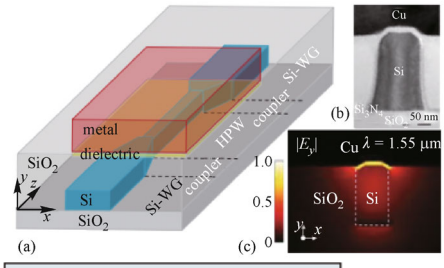	experiment	structure: Cu-SiO_2-Si λ: 1550 nm waveguide width: 160 nm loss: 0.122 dB/μm
[52]	2012	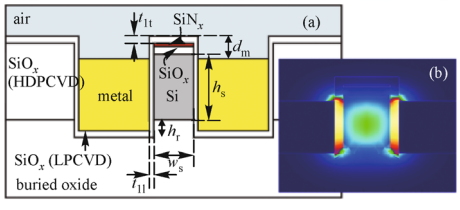	experiment	structure: Cu-SiO_x-Si-SiO_x-Cu λ: 1554 nm/1318 nm Si-core width: 160 – 220 nm loss: 0.2 – 0.3 dB/μm
[57]	2013	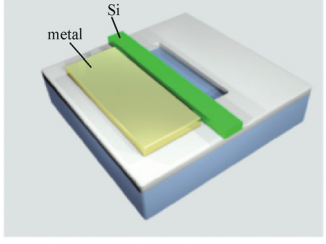	experiment	structure: Ag-air-Si λ: 1550 nm Si width: 400 nm loss: 0.14 dB/μm

(*Continued*)

Ref.	year	configuration	theory/ experiment	features
[56]	2013	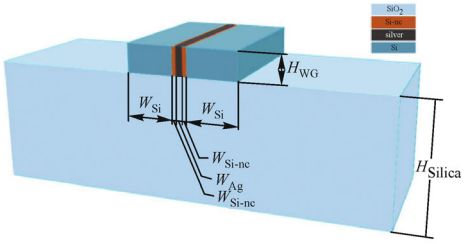	theory	structure: Si-Si:nc-Ag-Si-nc-Si λ: 1550 nm slot size: 150 nm × 200 nm loss: 3×10^{-4} dB/μm
[38]	2013	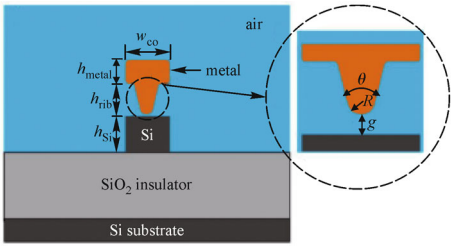	theory	structure: Ag-air-Si λ: 1550 nm A_{eff}: 2.8×10^{-6} λ^2 L_{prop}: 2.6 μm

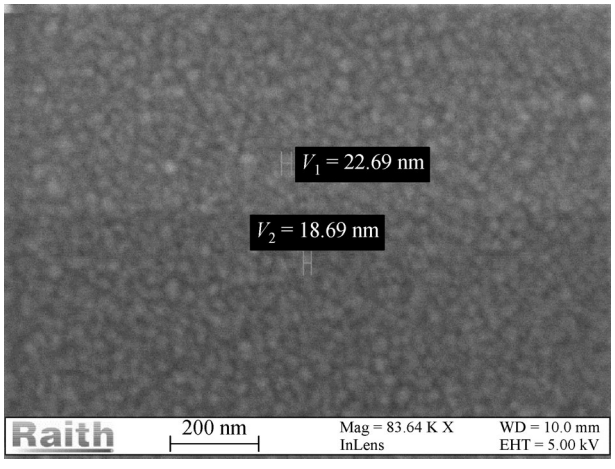

Fig. 3 SEM picture for a sputtering silver surface

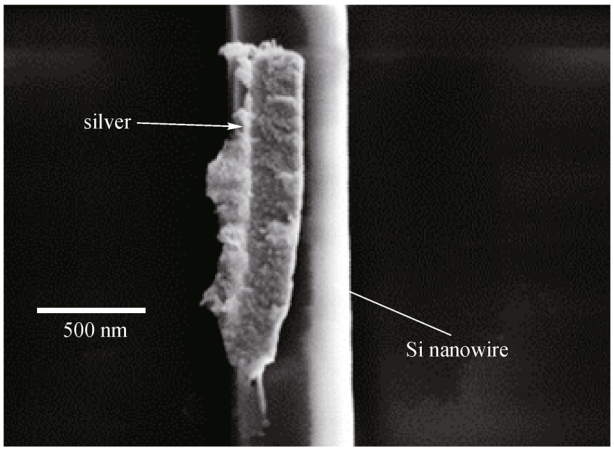

Fig. 4 SEM picture for a silicon hybrid nanoplasmonic waveguide with dropped metal [109]

standard SOI wafer can be used for this hybrid plasmonic waveguide and the SOI-compatibility makes the fabrication simplified. A 250 nm-wide silicon hybrid nanoplasmonic waveguide with such a structure was fabricated in 2010 [45], and the measured propagation length is about 40 μm with a gold cap, which agrees well with the calculation results. For the fabrication of a silicon hybrid nanoplasmonic waveguide, a challenge is to adhere the narrow metal strip on the SiO_2 film tightly. The process of the metal patterning should be careful. Otherwise, the metal strip might be lift-off, as shown in Fig. 4 [109]. A potential solution for this issue is to use the modified structure with a reversed metal ridge on the top for a silicon hybrid nanoplasmonic waveguide, as shown in Fig. 5(a) [47]. Figure 5(b) shows the field profile in a hybrid plasmonic waveguide. It can be seen that there is a significant field enhancement, which is similar to that shown in Ref. [21]. This type of silicon hybrid nanoplasmonic waveguide has been researched theoretically [46] as well experimentally [65]. The measured propagation loss of the fabricated silicon hybrid nanoplasmonic waveguide with copper is ~0.122 dB/μm for a 160 nm-wide waveguide [65]. In Ref. [48], Goykhman et al. demonstrated a silicon hybrid nanoplasmonic waveguide fabricated with the local oxidization process and the measured propagation loss is about 105 cm^{-1} for a 310 nm-wide waveguide.

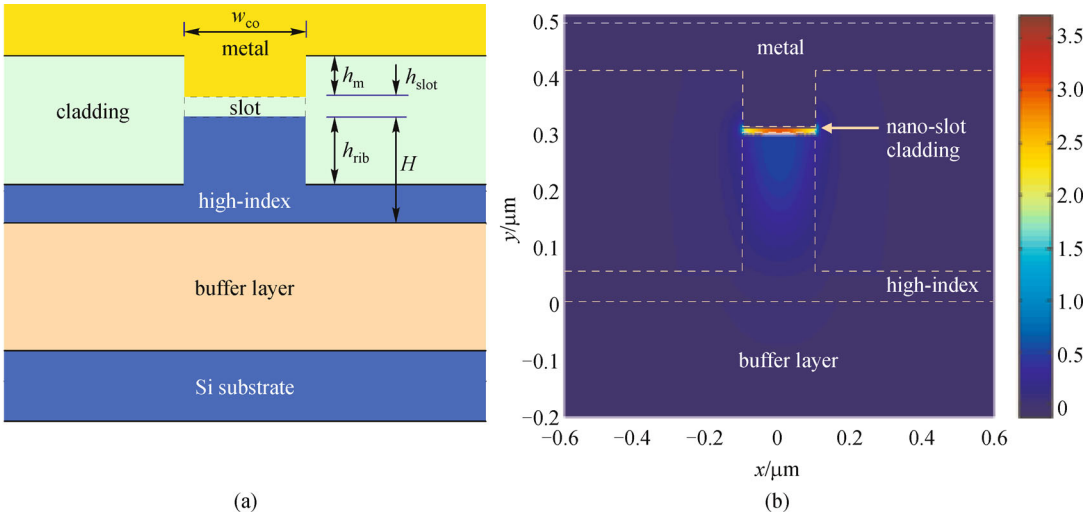

Fig. 5 (a) Cross section of a hybrid plasmonic waveguide with an inverted metal rib; (b) field distribution in a hybrid plasmonic waveguide with the following parameters: $n_H = 3.455$, $n_L = 1.445$, $n_{metal} = 0.1453 + 11.3587i$, $H = 300$ nm, $h_{rib} = 250$ nm, $h_{slot} = 10$ nm, $h_m = 100$ nm, and $w_{co} = 200$ nm [47]

2.3 Silicon hybrid nanoplasmonic waveguides for TE polarization

Silicon hybrid nanoplasmonic waveguide is usually designed for TM polarization, as shown above. In Ref. [49], we proposed a CMOS-compatible hybrid nanoplasmonic waveguide working for TE polarization, as shown Fig. 6(a). There are double nano-slots formed at both sides of the Si rib while the SiO_2 layer at the top of the Si rib is relatively thick to minimize the metal absorption. When the SiO_2 layer at both sides of the Si rib is thick (e.g., 0.5 μm-thick) and the Si rib is relatively wide (e.g., 400 nm), the fundamental mode field is confined well in the Si region and consequently the metal layer will hardly influence the mode field distribution. In this case, the present structure behaves like a regular SOI nanowire. However, the metal layer will give a significant influence to the guided mode when the SiO_2 thickness becomes small (e.g., < 50 nm). Figure 6(b) shows the calculated field distribution of the major-component $E_x(x, y)$ for the quasi-TE fundamental mode. The field distributions $E_x(x, y_0)$ and $E_x(x_0, y)$ are also shown. It can be seen that the present hybrid plasmonic waveguide provides a very good light confinement even when the waveguide core is as small as 50 nm (or even smaller). The field at the two 10 nm-SiO_2 nano-slots is enhanced greatly, which is similar to that shown in Fig. 5. In the present hybrid plasmonic waveguide, the double nano-slots help to

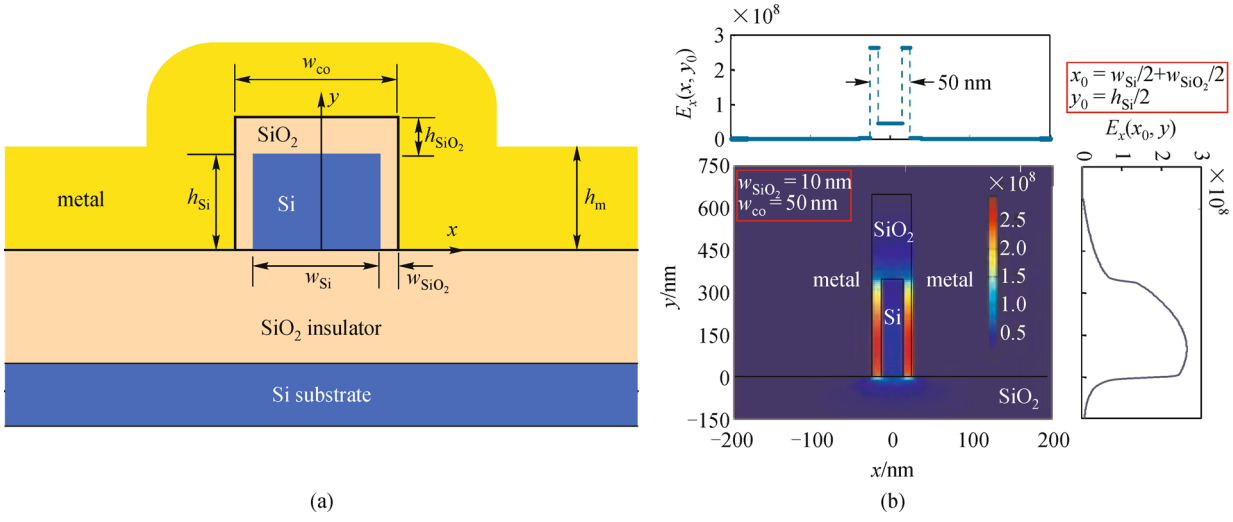

Fig. 6 (a) Cross section of a hybrid plasmonic waveguide with double low-index slots; (b) field distribution for the major component $E_x(x, y)$ of the quasi-TE fundamental mode when $w_{co} = 50$ nm and $w_{SiO_2} = 10$ nm. Here the field distributions $E_x(x_0, y)$ and $E_x(x, y_0)$ are also shown. Here $x_0 = w_{Si}/2 + w_{SiO_2}/2$ and $y_0 = h_{Si}/2$ [49]

achieve a very high power confinement factor at the low-index regions even when the slot area is very small. The theoretical analysis has shown that there is a very high power density in the SiO_2 nano-slots, e.g., $> 120\ \mu m^{-2}$ when $w_{SiO_2} = 10$ nm. The effective area A_{eff} is as small as $0.007\ \mu m^2$ for a 50 nm-wide waveguide with double 10-nm slots. This kind of silicon hybrid nanoplasmonic waveguide with double nano-slots working for TE polarization [49–55] has been investigated extensively. For example, Zhu et al. demonstrated the fabricated Cu-SiO_2-Si-SiO_2-Cu hybrid plasmonic waveguides has a loss of < 1dB/μm loss even when the silicon core width is as small as 21 nm [54]. The developed devices (like resonators, modulators) will be reviewed in Section 4.

In addition to the popular structures of silicon hybrid nanoplasmonic waveguides shown in Table 1, various novel designs have been presented more recently for realizing hybrid plasmonic waveguides with e.g., an additional semiconductor strip [28], multiple layers [29–31], angled sidewalls [32–34], a trench [35] and a silver nanowire [36]. Some extremely compact silicon hybrid nanoplasmonic waveguides have also been presented [37–39]. In Ref. [37], a hybrid plasmonic waveguide with a silicon cylindrical nanowire placed on a metal rib is proposed to achieve a sport size of 4.2 nm × 2.1 nm as well as a 38 μm-long propagation distance. In Ref. [38], the model with the nonlocal effect is used in the analysis for an ultrasmall small hybrid plasmonic waveguide.

According to the reported theoretical and experimental results for various silicon hybrid nanoplasmonic waveguides, it can be seen that silicon hybrid nanoplasmonic waveguides can confine light tightly in nano-scale and the propagation losses have been also verified to be acceptably low, which provides a good platform to realize ultrasmall functionality devices.

3 Silicon hybrid nanoplasmonic devices

3.1 Ultra-sharp bending of silicon hybrid nanoplasmonic waveguides

Figures 7(a)–7(d) show the electrical field distribution $E_y(x,y)$ of the TM fundamental mode for silicon hybrid nanoplasmonic waveguides with different bending radii R.

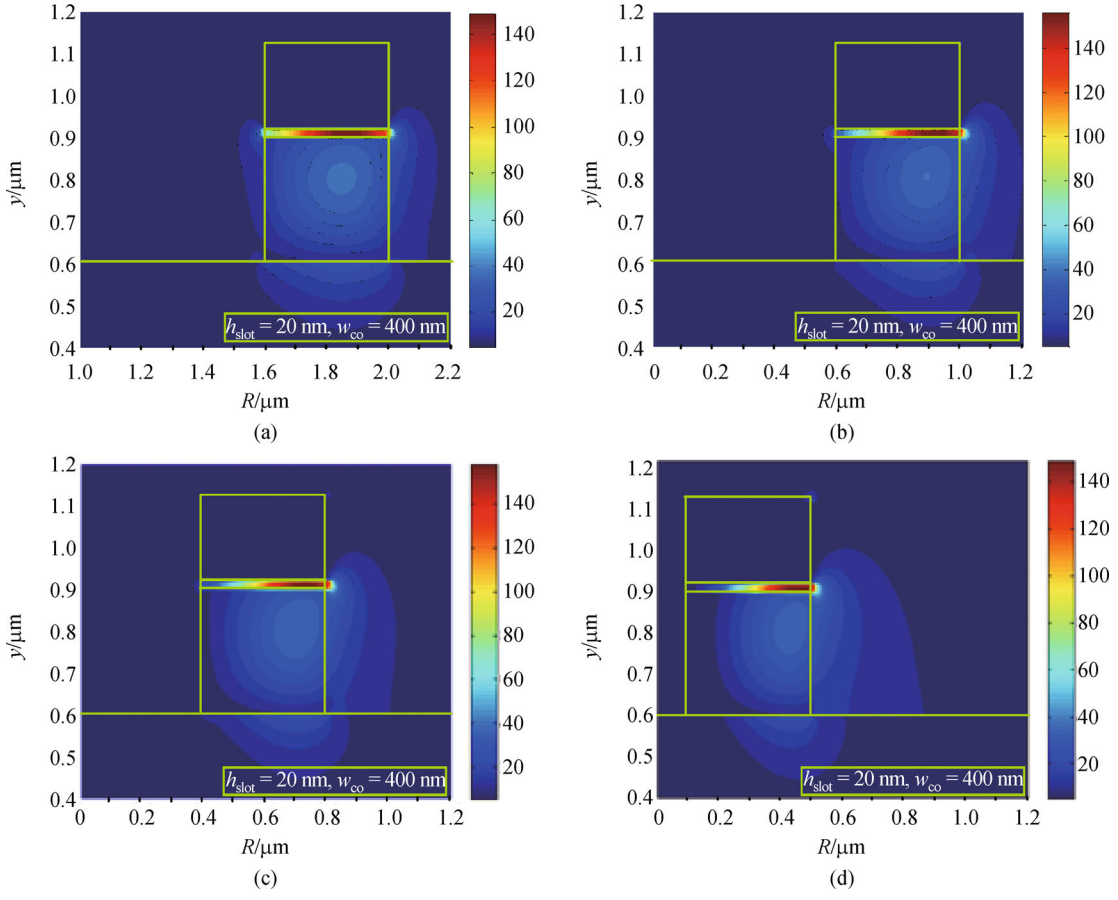

Fig. 7 Electrical field distribution $E_y(x, y)$ for the cases of (a) $R = 2$ μm, (b) $R = 1$ μm, (c) $R = 800$ nm, (d) $R = 500$ nm. The other parameters are: $h_{slot} = 20$ nm, $w_{co} = 400$ nm [71]

From these figures, it can be seen that there is a field enhancement in the low-index slot region and the light is still confined in the slot region very well even for the bending radius as small as 500 nm (about only 1/3 of the operation wavelength). This is due to the strong light confinement in silicon hybrid nanoplasmonic waveguides [71]. When the radius decreases, the peak of the electrical field shifts outward gradually, as predicted. This causes less field interaction with the inner sidewall, which helps to achieve low scattering loss.

Figures 8(a)–8(c) show the calculated loss for a 90°-bending hybrid plasmonic waveguide [71]. The loss is contributed by the intrinsic loss due to the metal absorption (which is proportional to the bending radius) as well as the leakage due to the bending (which increases exponentially as the bending radius decreases). Therefore, there is an optimal bending radius R_{opt}, which gives a minimal total loss for a 90°-bending, as shown in Figs. 8(a)–8(c). The bending loss for other silicon hybrid nanoplasmonic waveguides has also been studied. For example, Shin et al. gave an analysis for a metal-insulator-silicon-insulator-metal hybrid plasmonic waveguide and the calculated loss for a direct bend with a 220 nm-wide silicon core is 4.5 dB [70]. For Cu-SiO_2-Si-SiO_2-Cu hybrid plasmonic waveguides [64], the measured bending loss is about 0.73 dB/turn ($R = 0$) when the silicon core width is ~64 nm, which agrees well with the theoretical estimation. The ability for sharp bending makes silicon hybrid nanoplasmonic waveguide very promising to realize ultra-dense devices for photonic integration.

3.2 Optical couplers/splitters

The ultra-sharp bending can dramatically diminish the overall size of some basic elements based on silicon hybrid nanoplasmonic waveguides (e.g., power splitters/couplers) since 90°-bends or S-bends usually are used as the access parts. In Ref. [68], we presented the design for several types of power splitters with sub-μm^2 footprints based on a multimode interference (MMI) structures, as well as Y-branches, as shown in Figs. 9(a) and 9(b). The designed sub-μm^2 power splitter were also shown to work well in a broad wavelength range (1.25 – 1.7 μm), since the silicon hybrid nanoplasmonic waveguide bending can achieve low loss (e.g., < 0.12 dB/90° with an 800 nm radius) in such a broad band [71]. The experimental results for the ultrasmall power splitters based on the metal-SiO_2-Si-SiO_2-metal hybrid plasmonic waveguides were demonstrated in Ref. [54] and the measured loss for a fabricated 1 × 2 power splitter is ~1.4 dB (which is consistent with the

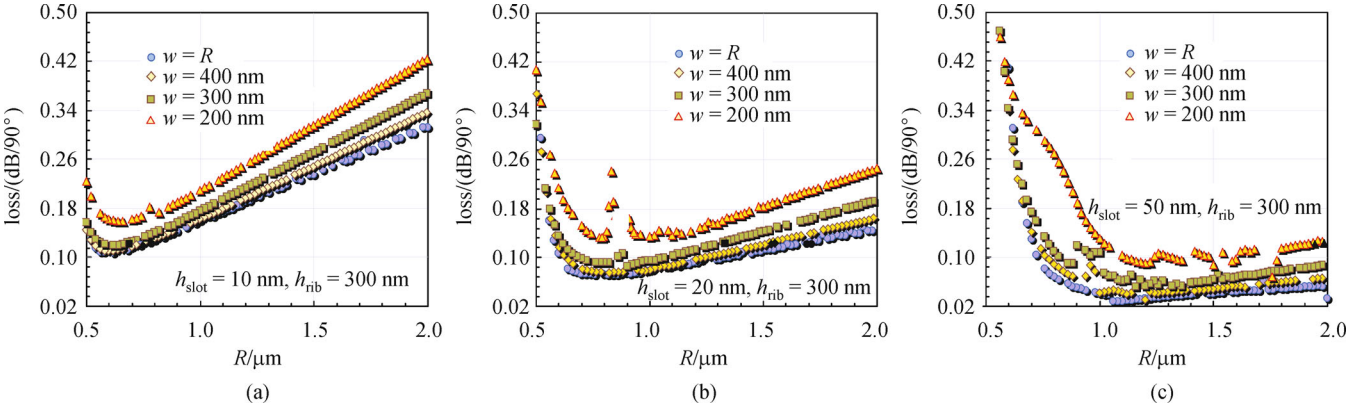

Fig. 8 Calculated bending loss for bent hybrid plasmonic waveguides (at 1550 nm). (a) h_{slot} = 10 nm; (b) h_{slot} = 20 nm; (c) h_{slot} = 50 nm [71]

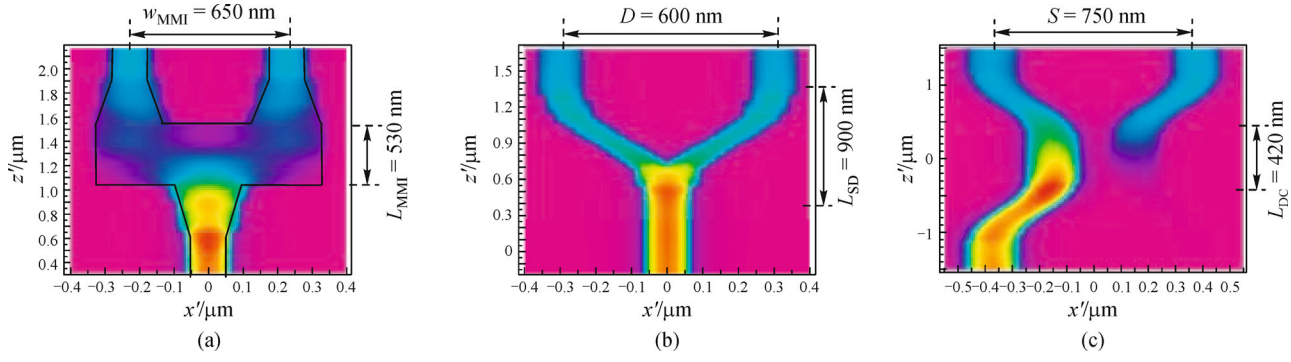

Fig. 9 (a) 1 × 2 3 dB MMI power splitter; (b) 1 × 2 3 dB Y-branch power splitter; (c) 1 × 2 3 dB DC

calculation result). Ultracompact directional couplers (DCs) based on silicon hybrid nanoplasmonic waveguides have also been realized in Refs. [40,59,61–63] (see Fig. 9 (c)) and the DC demonstrated in Ref. [40] has a coupling length as short as only 1.55 μm with arm widths of ~170 nm.

3.3 Ultrasmall resonators

As a versatile element for photonic integrated circuits, optical resonators have been attracting lots of attention for many applications, e.g., light sources [110], optical filters [111], optical modulators/switches [112], optical sensing [113], nonlinear optics [114], etc. As mentioned above, a silicon hybrid nanoplasmonic waveguide enables very sharp bending and thus it is promising to develop ultracompact resonators. Table 2 gives a summary for the developed silicon hybrid nanoplasmonic waveguide resonators, including microring resonators, micro-donut resonators, as well as micro-disk resonators.

It can be seen that the demonstrated silicon hybrid nanoplasmonic waveguide resonators have subwavelength or even submicron bending radius and the Q-factor is at the order of $10^2 - 10^3$. The Purcell factor is expected to be pretty high because of the ultrasmall volume, which is useful for the applications of single photon source, lasing or light-matter interactions. For example, the hybrid-plasmonic microdisk presented in Ref. [77] is with a bending radius ~890 nm and has a Purcell factor as high as 1824. In Ref. [71], we proposed a submicron-donut resonator, which has a pure dielectric access waveguide so that a long-distance optical interconnect is enabled and no additional mode converter is needed to combine the hybrid plasmonic circuits and the pure dielectric waveguides. The temperature-dependence of a silicon hybrid nanoplasmonic waveguide resonator has been analyzed [73] and an athermal resonator is achieved with the assistance of TiO_2 which has a negative thermal-optical coefficient [74]. Silicon hybrid nanoplasmonic waveguides have also been used to realize photonic-crystal cavities [78–80]. The cavity designed in Ref. [79] has a giant Q/V value (~60000 λ^{-3}), which offers a great opportunity to enhance the light-matter interaction.

3.4 Polarization handling devices

Surface plasmonic waveguides are well known for the strong polarization dependence and usually there are surface plasmonic modes supported for only one polarization. Similarly silicon hybrid nanoplasmonic waveguide also has very strong polarization-dependence. Figure 10 shows the dominant electric field for the TE fundamental (TE_0) mode and TM fundamental (TM_0) mode. It can be seen that the TE_0 modal field is mainly confined in the silicon region while the TM_0 modal field has a peak enhancement in the SiO_2 nanoslot. This distinction makes it possible to realize polarization handling devices conveniently, including polarizers, polarization beam splitters (PBSs) as well as polarization rotators, which is very useful for many applications [115].

Polarizer is useful to improve the extinction ratio of polarized light and in recent years various ultra-short polarizers based on silicon hybrid nanoplasmonic waveguides have been proposed [81 – 86]. In 2012, the polarization-dependence of the mode coupling [84] as well as the mode absorption loss [86] in a silicon hybrid nanoplasmonic waveguide has been utilized to realize compact TE-pass polarizers. For a 30 μm-long polarizer demonstrated, the extinction ratio is ~23 dB and the insertion loss is about 2 dB. Huang et al. proposed a TE-pass polarizer with a 16 dB extinction ratio and a 2.2 dB insertion loss by using a silicon hybrid nanoplasmonic waveguide with double nano-slots [85]. More recently, an ultrasmall TE-pass silicon-hybrid-plasmonic-waveguide polarizer with a broadband (>200 nm band for 15 dB extinction ratio) is proposed with a Bragg grating structure [83]. In a similar way, TM-pass polarizers can also be realized with silicon hybrid nanoplasmonic waveguide [81,82], which plays important role for some applications to improve the extinction ratio of TM polarized light.

To realize compact PBSs, which are used to separate or combine TE and TM polarizations, an asymmetrical coupling system has been proved to be a good candidate [115]. Particularly, asymmetrical couplers consisting of a silicon hybrid nanoplasmonic waveguide and silicon nanowires has been proposed to realize ultrasmall PBS [87–91]. The PBS length can be even shortened with a MMI coupler proposed in Ref. [92]. In this design, a metal strip is partially covered on the MMI section to form a Si hybrid plasmonic waveguide, as shown in Fig. 11(a). For TM polarization, the fundamental mode in the MMI section is excited dominantly due to the hybrid plasmonic effect so that the MMI effect does not happen almost. Consequently the TM-polarized light outputs from the through port (as shown in Fig. 11(b)). On the other hand, for TE polarization, the metal on the top influences the light propagation very slightly because there is no hybrid plasmonic effect, and thus the MMI length is chosen optimally to form a mirror image at the cross port (as shown in Fig. 11(b)). With such a design, the MMI section for the PBS is as short as only 1.1 μm, and the PBS has a broad bandwidth of ~80 nm for an extinction ratio of >10 dB. The insertion losses are only 0.32 and 0.88 dB for TE and TM polarizations, respectively.

Polarization rotation is another key to realize polarization-handling [115]. Generally, an on-chip polarization rotator based on pure-dielectric optical waveguides can be realized with the mechanism of the mode evolution [116] as well as the hybrid-mode interference [117]. Similarly, for the case with silicon hybrid nanoplasmonic wave-

Table 2 Silicon hybrid nanoplasmonic waveguide resonators

Ref.	year	structure	R	extinction ratio	Q	FSR
[71]	2011	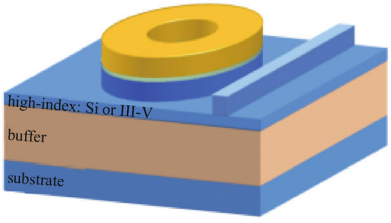	800 nm	30 dB	220	148 nm
[77]	2011	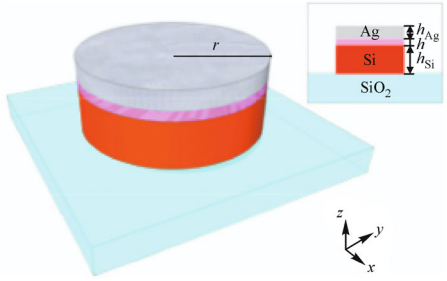	890 nm	–	648	140 nm
[75]	2011	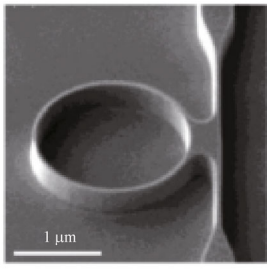	910 nm	28 dB	638	143 nm
[65]	2012	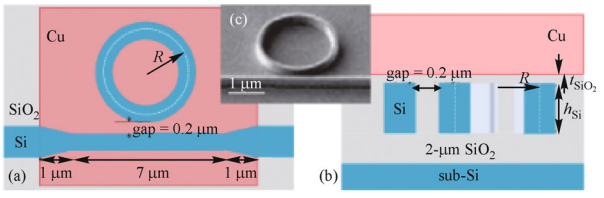	1.09 μm	13.7 dB	63	106 nm
[76]	2013	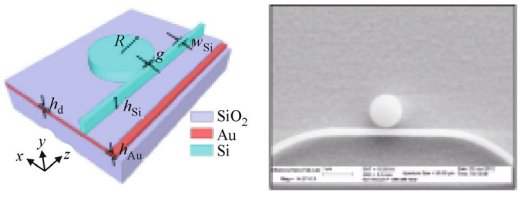	522 nm	12.4 dB	110	210 nm

guides, low-loss compact polarization rotators [93–95] can also be obtained by utilizing the mode evolution [94], and the hybrid-mode interference [95]. For example, a 3.2 μm-long polarization rotator is presented with a conversion efficiency of 99.5% and an insertion loss of 1.38 dB [95].

As a summary, it can be concluded that a silicon hybrid nanoplasmonic waveguide provide a very promising platform to realize ultrasmall on-chip polarization-handling devices, which is attractive for the future large-scale photonic integrated circuits.

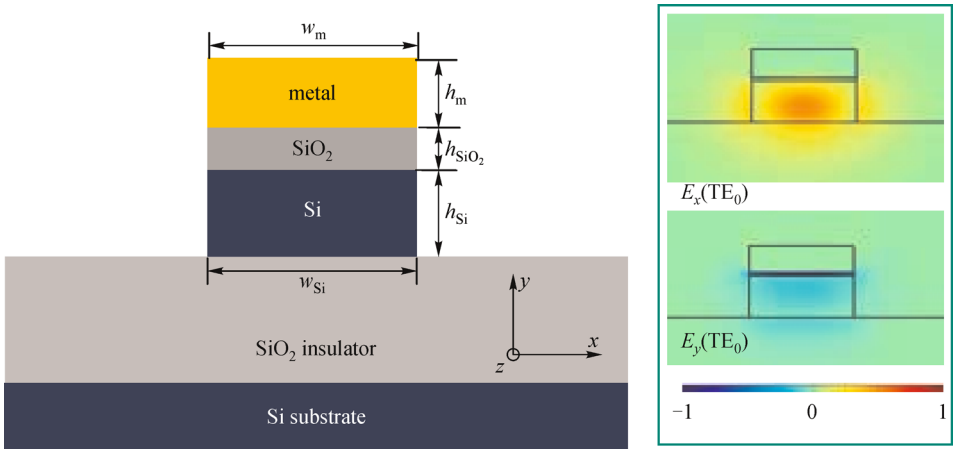

Fig. 10 Cross section of a silicon hybrid nanoplasmonic waveguide and the filed distributions for the TE_0 and TM_0 modes

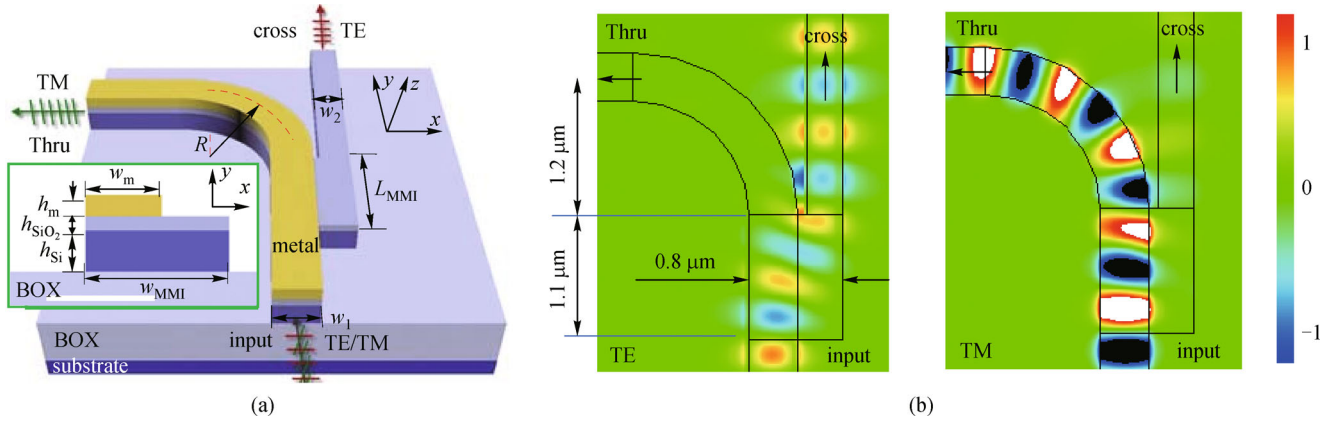

Fig. 11 Configuration (a) and light propagation (b) of a PBS with a MMI coupler on Si HPW platform [92]

4 Discussion on the issue and applications of silicon hybrid nanoplasmonic waveguides

4.1 Loss issue

Even though a silicon hybrid nanoplasmonic waveguide has a relatively low loss and a relatively long propagation distance is enabled, the intrinsic loss of the metal is still a hinder for the applications of silicon hybrid nanoplasmonic waveguides.

A potential solution is using silicon hybrid nanoplasmonic waveguides locally on the chip with the assistance from low-loss pure dielectric waveguides (SOI nanowires [118]) for long-distance interconnects. This kind of hybrid integration has been used to realize ultrasmall devices [71,87–92]. For example, we proposed a silicon hybrid nanoplasmonic resonant donut with pure dielectric access waveguides [71]. To realize the seamless integration between hybrid plasmonic circuits and silicon nanophotonic circuits, there are usually two ways for light coupling, e.g., the butt-coupling [67,96,119] and the evanescent-coupling [63,120,121]. The butt-coupling way has an efficiency of $>55\%$ in a wavelength band as large as 200 nm [96]. For the evanescent-coupling way, one should design the silicon hybrid nanoplasmonic waveguide and the silicon nanowire according to the phase matching condition and the coupling efficiency can be up to 94% [63].

Another potential way to overcome the intrinsic loss of hybrid plasmonic waveguides is introducing gain medium. Table 3 gives a brief summary for gain mediums used in the gain-assisted plasmonic waveguides [47,122 – 133]. In Ref. [122], a net gain of 85.5 dB/cm for long-range surface plasmonic waveguides has been demonstrated by using a dipolar gain medium with a gain coefficient of ~420 cm^{-1}. For silicon hybrid nanoplasmonic waveguides, either high-index or low-index gain medium could be used in the high-index region or in the low-index region respectively. For example, semiconductor materials have been used to act as the high-index layer as well as the gain medium for hybrid plasmonic waveguide [134–136]. Particularly, for a silicon hybrid nanoplasmonic waveguide with a metal strip on a

slab waveguide [21], the theoretical gain coefficient required to compensate the metal loss can be as low as 3.8 cm^{-1} [137], which makes it possible to achieve silicon hybrid nanoplasmonic waveguides with net gain. When a net gain is achieve with the assistance of gain medium, a deep subwavelength laser based on hybrid plasmonic waveguides has been realized [43], and the laser can operates even at the room temperature [138]. As shown in Table 3, there are also some options of low-index gain medium available for silicon hybrid nanoplasmonic waveguides, e.g., silicon nano-crystals [132], Er-doped oxide [124,125] or polymer with quantum dots [129]. The theoretical analysis in Ref. [47] shows that it is possible to compensate the intrinsic loss and even achieve a pure gain with a moderate gain medium.

4.2 Applications of silicon hybrid nanoplasmonic waveguides

The field enhancement in the low-index nano-slot makes silicon hybrid nanoplasmonic waveguides very useful for many applications (e.g., optical modulation, optical nonlinearity, optical sensing, optical force, etc), when filling some functionality medium into the nano-slot region.

For example, in order to realize optical modulator, the nano-slot region can be filled in with some electro-optic (EO) material like HfO_2 [97], Vandium dioxide [98], and EO polymer [99,100]. For EO-polymer, the EO coefficient can be very high (~500 pm/V [101]). The field enhancement in the nano-slots filled by EO-polymer helps obtain an ultra-short π-phase-shifter (e.g., ~13 μm-long with a 2.5 V voltage [102]). The compactness makes it possible to achieve a very high modulation speed of up to 100 GHz as well as very low power consumption of 9 fJ/bit [102]. The power consumption can be even reduced further to e.g. 5 fJ/bit (~100 GHz) by utilizing a silicon hybrid nanoplasmonic resonator (e.g., a nano-disk resonant, R = 510 nm) [100]. When the low-index material is with negative thermal coefficient, an athermal modulator with silicon hybrid nanoplasmonic waveguides can also be achieved [139]. The temperature-insensitivity of an optical modulator indeed benefits from the strong confinement in the low-index region with negative thermal coefficient, regarding that the low-index layer (TiO_2) is as thin as ~ 58 nm.

When the nano-slots are filled with some nonlinear optical material (e.g., nonlinear polymer), an enhanced optical nonlinear effect can be obtained. Zhou et al. presented a silicon hybrid nanoplasmonic waveguide offering an ultra-high nonlinear coefficient $\gamma = 4.7 \times 10^9\ W^{-1}\cdot km^{-1}$, which is 4 orders larger than conventional silicon waveguides [25]. An optical parametric amplifier (OPA) is also presented theoretically with a signal gain 14 dB over a 200 nm broad-band [140]. With the nonlinearity of a silicon hybrid nanoplasmonic waveguide, one can also achieve efficient phase-matched second harmonic generation (SHG) from mid-infrared (IR) to near-IR and the SHG yield is as large as 8.8% for a pumping power of 100 mW [141]. In Refs. [142] and [143], more details for the nonlinearity in the silicon hybrid nanoplasmonic waveguides have been given. The enhanced nonlinearity in hybrid plasmonic waveguide enables all-optical switching [144], optical logic gate [145], and signal-format converters [146].

A silicon hybrid nanoplasmonic waveguide is also advantageous for optical sensing because of the high sensitivity due to the field enhancement [104,105]. A subwavelength resonator based on silicon hybrid nanoplasmonic waveguides has been proposed as a biosensor [106] and the sensitivity is ~580 nm/RIU, which is much higher than that for a dielectric nanoslot-waveguide resonator. The compactness of such a sensor also makes it possible to achieve ultra-high integration density and

Table 3 Gain reported in literatures [47]

Ref.	gain medium	gain	wavelength
[122]	IR140 dye molecules (Sigma Aldrich)	360 cm^{-1}	882 nm
[123]	PMMA with Rhodamine 6G dye (R6G)	420 cm^{-1}	594 nm
[124]	Er-doped phosphate glass	1 cm^{-1}	1532 nm
[125]	Er-doped Al_2O_3	0.3 cm^{-1}	1530 nm
[126]	sulfide (PbS) QDs	150 cm^{-1}	1525 nm
[127]	GaInAsP	1200 cm^{-1}	1500 nm
[128]	PbS semiconductor quantum dots	1700 cm^{-1}	1250 nm
[129]	PMMA with PbS QDs	17 cm^{-1}	1160 nm
[130]	dye solution	–	633 nm
[131]	PbS QDs	200 cm^{-1}	860 nm
[132]	silicon nanocrystals	100 cm^{-1}	800 nm
[133]	MDMO-PPV:PSF	90 cm^{-1}	600 nm

high spatial resolution for a sensor array.

Recently, it has shown that enhanced optical forces can be realized by using silicon hybrid nanoplasmonic waveguides [57,107,108]. In comparison with pure dielectric optical waveguides, the optical force in silicon hybrid nanoplasmonic waveguides is enhanced several times, which makes it useful to realize nano-scale optical tweezers [107].

More applications for hybrid plasmonic waveguides are still being explored, including light concentration [147], wavelength division multiplexing (WDM) system [148], electrically induced transparency (EIT) [149], optical filters [150], light controlling [151–153], meta-material [154], detectors [155] and terahertz waveguides [156]. These attempts to extend the applications of silicon hybrid nanoplasmonic waveguide are beneficial to develop complicated ultra-dense integrated photonic circuits in the future.

5 Conclusions

In this paper, we have given a review for recent progresses on silicon hybrid nanoplasmonic waveguides and devices. It has shown that silicon hybrid nanoplasmonic waveguides have attracted lots of attention in the past years (especially since 2009) because of the ability to achieve a nano-scale confinement of light as well as long propagation distance (~10^2 μm). This is beneficial for realizing ultra-dense photonic integrated circuits in the future. For example, sub-μm^2 silicon hybrid nanoplasmonic integrated devices have been demonstrated, including power splitters, nano-donut resonators, polarization-handling devices. As a general solution for the loss issue of hybrid plasmonic waveguides, low-index or high-index gain medium have been introduced to compensate the intrinsic loss. In comparison with the conventional nanoplasmonic waveguide, an advantage of hybrid plasmonic waveguide is that the gain medium does not need a high gain coefficient because of the relatively low intrinsic loss, which makes loss compensation feasible in practice. The combination of silicon hybrid nanoplasmonic waveguides for local functionality elements with ultra-small footprints and low-loss pure dielectric waveguides for long-distance interconnect also provides a promising way to alleviate the loss issue, which has been used for silicon hybrid nanoplasmonic resonators, PBSs, etc. The field enhancement in a silicon hybrid nanoplasmonic waveguide makes it very useful. The application of silicon hybrid nanoplasmonic waveguides has been extended to the fields including nonlinear optics, optical modulation, optical sensing, and optical force. It is expected to explore more applications for silicon hybrid nanoplasmonic waveguides, like active plasmonics, quantum plasmonics, etc.

Acknowledgements This project was partially supported by the National Natural Science Foundation of China (Grant No. 11374263), the National High-Tech R&D program of China (863 program) (No. 2011AA010301), Zhejiang Provincial Grant (No. Z201121938), the Doctoral Fund of Ministry of Education of China (No. 20120101110094).

References

1. Tsuchizawa T, Yamada K, Fukuda H, Watanabe T, Takahashi J, Takahashi M, Shoji T, Tamechika E, Itabashi S, Morita H. Microphotonics devices based on silicon microfabrication technology. IEEE Journal on Selected Topics in Quantum Electronics, 2005, 11(1): 232–240
2. Almeida V R, Xu Q, Barrios C A, Lipson M. Guiding and confining light in void nanostructure. Optics Letters, 2004, 29(11): 1209–1211
3. Thylén L, Qiu M, Anand S. Photonic crystals—a step towards integrated circuits for photonics. ChemPhysChem, 2004, 5(9): 1268–1283
4. Goto T, Katagiri Y, Fukuda H, Shinojima H, Nakano Y, Kobayashi I, Mitsuoka Y. Propagation loss measurement for surface plasmon-polariton modes at metal waveguides on semiconductor substrates. Applied Physics Letters, 2004, 84(6): 852–854
5. Charbonneau R, Lahoud N, Mattiussi G, Berini P. Demonstration of integrated optics elements based on long-ranging surface plasmon polaritons. Optics Express, 2005, 13(3): 977–984
6. Zia R, Selker M D, Catrysse P B, Brongersma M L. Geometries and materials for subwavelength surface plasmon modes. Journal of the Optical Society of America. A, Optics, Image Science, and Vision, 2004, 21(12): 2442–2446
7. Wang B, Wang G P. Surface plasmon polariton propagation in nanoscale metal gap waveguides. Optics Letters, 2004, 29(17): 1992–1994
8. Tanaka K, Tanaka M. Simulations of nanometric optical circuits based on surface plasmon polariton gap waveguide. Applied Physics Letters, 2003, 82(8): 1158–1160
9. Tanaka K, Tanaka M, Sugiyama T. Simulation of practical nanometric optical circuits based on surface plasmon polariton gap waveguides. Optics Express, 2005, 13(1): 256–266
10. Kusunoki F, Yotsuya T, Takahara J, Kobayashi T. Propagation properties of guided waves in index-guided two-dimensional optical waveguides. Applied Physics Letters, 2005, 86(21): 211101-1–211101-3
11. Pile D F P, Gramotnev D K. Channel plasmon-polariton in a triangular groove on a metal surface. Optics Letters, 2004, 29(10): 1069–1071
12. Bozhevolnyi S I, Volkov V S, Devaux E, Laluet J Y, Ebbesen T W. Channel plasmon subwavelength waveguide components including interferometers and ring resonators. Nature, 2006, 440(7083): 508–511
13. Pile D F P, Gramotnev D K. Plasmonic subwavelength waveguides: next to zero losses at sharp bends. Optics Letters, 2005, 30(10): 1186–1188
14. Xiao S S, Liu L, Qiu M. Resonator channel drop filters in a plasmon-polaritons metal. Optics Express, 2006, 14(7): 2932–2937

15. Liu L, Han Z H, He S L. Novel surface plasmon waveguide for high integration. Optics Express, 2005, 13(17): 6645–6650
16. Veronis G, Fan S H. Bends and splitters in metal-dielectric-metal subwavelength plasmonic waveguides. Applied Physics Letters, 2005, 87(13): 131102-1–131102-3
17. Zia R, Schuller A J, Chandran A, Brongersma L M. Plasmonics: the next chip-scale technology. Materials Today, 2006, 9(7–8): 21–27
18. Alam M Z, Meier J, Aitchison J S, Mojahedi M. Super mode propagation in low index medium. In: Proceedings of Quantum Electronics and Laser Science Conference. Baltimore, 2007, JThD112
19. Oulton R F, Sorger V J, Genov D A, Pile D F P, Zhang X. A hybrid plasmonic waveguide for subwavelength confinement and long-range propagation. Nature Photonics, 2008, 2(8): 496–500
20. Fujii M, Leuthold J, Freude W. Dispersion relation and loss of subwavelength confined mode of metal-dielectric-gap optical waveguides. IEEE Photonics Technology Letters, 2009, 21(6): 362–364
21. Dai D X, He S. A silicon-based hybrid plasmonic waveguide with a metal cap for a nano-scale light confinement. Optics Express, 2009, 17(19): 16646–16653
22. Dai D X, Yang L. Proposal of a thermally-tunable silicon-on-insulator microring resonator filter. In: Proceedings of Asia Optical Fiber Communication & Optoelectrnic Exposition & Conference. Shanghai, 2007, 582–583
23. Feng N N, Brongersma M L, Negro L D. Metal-dielectric slot-waveguide structures for the propagation of surface plasmon polaritons at 1.55 μm. IEEE Journal of Quantum Electronics, 2007, 43(6): 479–485
24. Wang Z, Dai D X, Shi Y, Somesfalean G, Holmstrom P, Thylen L, He S, Wosinski L. Experimental realization of a low-loss nano-scale Si hybrid plasmonic waveguide. In: Proceedings of Optical Fiber Communication Conference. Los Angeles, 2011
25. Zhou G, Wang T, Pan C, Hui X, Liu F F, Su Y K. Design of plasmon waveguide with strong field confinement and low loss for nonlinearity enhancement. In: Group Four Photonics. Beijing, 2010
26. Chen L, Zhang T, Li X, Huang W. Novel hybrid plasmonic waveguide consisting of two identical dielectric nanowires symmetrically placed on each side of a thin metal film. Optics Express, 2012, 20(18): 20535–20544
27. Tian J, Ma Z, Li Q, Song Y, Liu Z, Yang Q, Zha C L, Akerman J, Tong L M, Qiu M. Nanowaveguides and couplers based on hybrid plasmonic modes. Applied Physics Letters, 2010, 97(23): 231121-1–231121-3
28. Bian Y S, Zheng Z, Zhao X, Liu L, Su Y L, Liu J S, Zhu J S, Zhou T. Hybrid plasmonic waveguide incorporating an additional semiconductor stripe for enhanced optical confinement in the gap region. Journal of Optics, 2013, 15(3): 035503-1–035503-9
29. Bian Y S, Gong Q H. Multilayer metal-dielectric planar waveguides for subwavelength guiding of long-range hybrid plasmon polaritons at 1550 nm. Journal of Optics, 2014, 16(1): 015001-1–015001-12
30. Chen L, Li X, Wang G P, Li W, Chen S H, Xiao L, Gao D S. A silicon-based 3-D hybrid long-rang plasmonic waveguide for nanophotonic integrating. Journal of Lightwave Technology, 2012, 30(1): 163–168
31. Noghani M T, Samiei M H V. Analysis and optimum design of hybrid plasmonic slab waveguides. Plasmonics, 2013, 8(2): 1155–1168
32. Bian Y S, Zheng Z, Zhao X, Liu L, Su Y L, Liu J S, Zhu J S, Zhou T. Hybrid plasmon polariton guiding with tight mode confinement in a V-shaped metal/dielectric groove. Journal of Optics, 2013, 15 (5): 055011-1–055011-6
33. Bian Y S, Gong Q. Low-loss hybrid plasmonic modes guided by metal-coated dielectric wedges for subwavelength light confinement. Applied Optics, 2013, 52(23): 5733–5741
34. Bian Y S, Gong Q. Low-loss light transport at the subwavelength scale in silicon nano-slot based symmetric hybrid plasmonic waveguiding schemes. Optics Express, 2013, 21(20): 23907–23920
35. Amirhosseini A, Safian R. A hybrid plasmonic waveguide for the propagation of surface plasmon polariton at 1.55 μm on SOI substrate. IEEE Transactions on Nanotechnology, 2013, 12(6): 1031–1036
36. Kou Y, Ye F W, Chen X F. Low-loss hybrid plasmonic waveguide for compact and high-efficient photonic integration. Optics Express, 2011, 19(12): 11746–11752
37. Hao R, Li E P, Wei X C. Two-dimensional light confinement in cross-index-modulation plasmonic waveguides. Optics Letters, 2012, 37(14): 2934–2936
38. Huang Q, Bao F, He S. Nonlocal effects in a hybrid plasmonic waveguide for nanoscale confinement. Optics Express, 2013, 21 (2): 1430–1439
39. Lu Q, Chen D, Wu G. Low-loss hybrid plasmonic waveguide based on metal ridge and semiconductor nanowire. Optics Communications, 2013, 289: 64–68
40. Lou F, Wang Z, Dai D, Thylen L, Wosinski L. Experimental demonstration of ultra-compact directional couplers based on silicon hybrid plasmonic waveguides. Applied Physics Letters, 2012, 100(24): 241105-1–241105-4
41. Alam M Z, Meier J, Aitchison J S, Mojahedi M. Propagation characteristics of hybrid modes supported by metal-low-high index waveguides and bends. Optics Express, 2010, 18(12): 12971–12979
42. Horvath C, Bachman D, Wu M, Perron D, Van V. Polymer hybrid plasmonic waveguides and microring resonators. IEEE Photonics Technology Letters, 2011, 23(17): 1267–1269
43. Oulton R F, Sorger V J, Zentgraf T, Ma R M, Gladden C, Dai L, Bartal G, Zhang X. Plasmon lasers at deep subwavelength scale. Nature, 2009, 461(7264): 629–632
44. Su Y, Zheng Z, Bian Y S, Liu Y, Liu J S, Zhu J S, Zhou T. Low-loss silicon-based hybrid plasmonic waveguide with an air nanotrench for sub-wavelength mode confinement. Micro & Nano Letters, 2011, 6(8): 643–645
45. Wu M, Han Z, Van V. Conductor-gap-silicon plasmonic waveguides and passive components at subwavelength scale. Optics Express, 2010, 18(11): 11728–11736
46. Bian Y S, Zheng Z, Zhao X, Liu L, Su Y L, Liu J S, Zhu J S, Zhou T. Nanoscale light guiding in a silicon-based hybrid plasmonic waveguide that incorporates an inverse metal ridge. Physica Status

Solidi A, 2013, 210(7): 1424–1428
47. Dai D X, Shi Y C, He S L, Wosinski L, Thylen L. Gain enhancement in a hybrid plasmonic nano-waveguide with a low-index or high-index gain medium. Optics Express, 2011, 19(14): 12925–12936
48. Goykhman I, Desiatov B, Levy U. Experimental demonstration of locally oxidized hybrid silicon-plasmonic waveguide. Applied Physics Letters, 2010, 97(14): 141106-1–141106-3
49. Dai D X, He S L. Low-loss hybrid plasmonic waveguide with double low-index nano-slots. Optics Express, 2010, 18(17): 17958–17966
50. Kwon M S. Metal-insulator-silicon-insulator-metal waveguides compatible with standard CMOS technology. Optics Express, 2011, 19(9): 8379–8393
51. Kim J T. CMOS-compatible hybrid plasmonic slot waveguide for on-chip photonic circuits. IEEE Photonics Technology Letters, 2011, 23(20): 1481–1483
52. Kwon M S, Shin J S, Shin S Y, Lee W G. Characterizations of realized metal-insulator-silicon-insulator-metal waveguides and nanochannel fabrication via insulator removal. Optics Express, 2012, 20(20): 21875–21887
53. Zhu S, Liow T Y, Lo G Q, Kwong D L. Fully complementary metal-oxide-semiconductor compatible nanoplasmonic slot waveguides for silicon electronic photonic integrated circuits. Applied Physics Letters, 2011, 98(2): 021107-1–021107-3
54. Zhu S, Liow T Y, Lo G Q, Kwong D L. Silicon-based horizontal nanoplasmonic slot waveguides for on-chip integration. Optics Express, 2011, 19(9): 8888–8902
55. Zuo X, Sun Z. Low-loss plasmonic hybrid optical ridge waveguide on silicon-on-insulator substrate. Optics Letters, 2011, 36(15): 2946–2948
56. Xiang C, Wang J. Long-range hybrid plasmonic slot waveguide. IEEE Photonics Journal, 2013, 5(2): 4800311-1–4800311-11
57. Li H, Noh J W, Chen Y, Li M. Enhanced optical forces in integrated hybrid plasmonic waveguides. Optics Express, 2013, 21 (10): 11839–11851
58. Xiao J, Liu J, Zheng Z, Bian Y, Wang G, Li S. Low-loss metal-insulator-semiconductor waveguide with an air core for on-chip integration. Optics Communications, 2012, 285(17): 3604–3607
59. Guan X, Chen P, Wang X, Wosinski L, Shi Y, Dai D. Ultrasmall directional coupler and disk-resonantor based on nano-scale silicon hybrid plasmonic waveguides. In: Proceedings of Asia Communications and Photonics Conference. Guangzhou, 2012
60. Song Y, Yan M, Yang Q, Tong L M, Qiu M. Reducing crosstalk between nanowire-based hybrid plasmonic waveguides. Optics Communications, 2011, 284(1): 480–484
61. Alam M Z, Caspers J N, Aitchison J S, Mojahedi M. Compact low loss and broadband hybrid plasmonic directional coupler. Optics Express, 2013, 21(13): 16029–16034
62. Noghani M T, Samiei M H V. Ultrashort hybrid metal-insulator plasmonic directional coupler. Applied Optics, 2013, 52(31): 7498–7503
63. Li Q, Song Y, Zhou G, Su Y K, Qiu M. Asymmetric plasmonic-dielectric coupler with short coupling length, high extinction ratio, and low insertion loss. Optics Letters, 2010, 35(19): 3153–3155
64. Zhu S, Lo G Q, Kwong D L. Components for silicon plasmonic nanocircuits based on horizontal Cu-SiO_2-Si-SiO_2-Cu nanoplasmonic waveguides. Optics Express, 2012, 20(6): 5867–5881
65. Zhu S, Lo G Q, Kwong D L. Experiment demonstration of vertical Cu-SiO_2-Si hybrid plasmonic waveguide components on an SOI platform. IEEE Photonics Technology Letters, 2012, 24(14): 1224–1226
66. Chu H S, Bai P, Li E P, Hoefer W R J. Hybrid dielectric-loaded plasmonic waveguide-based power splitter and ring resonator: compact size and high optical performance for nanophotonic circuits. Plasmonics, 2011, 6(3): 591–597
67. Song Y, Wang J, Yan M, Qiu M. Efficient coupling between dielectric and hybrid plasmonic waveguides by multimode interference power splitter. Journal of Optics, 2011, 13(7): 075002-1–075002-8
68. Wang J, Guan X, He Y, Shi Y, Wang Z, He S, Holmström P, Wosinski L, Thylen L, Dai D. Sub-μm^2 power splitters by using silicon hybrid plasmonic waveguides. Optics Express, 2011, 19(2): 838–847
69. Xiao J, Liu J, Zheng Z, Bian Y, Wang G. Design and analysis of a nanostructure grating based on a hybrid plasmonic slot waveguide. Journal of Optics, 2011, 13(10): 105001
70. Shin J S, Kwon M S, Lee C H, Shin S Y. Investigation and improvement of 90° direct bends of metal-insulator-silicon-insulator-metal waveguides. IEEE Photonics Journal, 2013, 5(5): 6601909-1–6601909-5
71. Dai D, Shi Y, He S, Wosinski L, Thylen L. Silicon hybrid plasmonic submicron-donut resonator with pure dielectric access waveguides. Optics Express, 2011, 19(24): 23671–23682
72. Chu H S, Akimov Y, Bai P, Li E P. Submicrometer radius and highly confined plasmonic ring resonator filters based on hybrid metal-oxide-semiconductor waveguide. Optics Letters, 2012, 37 (21): 4564–4566
73. Zhu S, Lo G Q, Kwong D L. Performance of ultracompact copper-capped silicon hybrid plasmonic waveguide-ring resonators at telecom wavelengths. Optics Express, 2012, 20(14): 15232–15246
74. Zhu S, Lo G, Kwong D L. Towards athermal nanoplasmonic resonators based on Cu-TiO_2-Si hybrid plasmonic waveguide. In: Proceedings of Optical Fiber Communication Conference/National Fiber Optic Engineers Conference. Anaheim, 2013
75. Zhu S, Lo G Q, Kwong D L. Experimental demonstration of horizontal nanoplasmonic slot waveguide-ring resonators with submicrometer radius. IEEE Photonics Technology Letters, 2011, 23(24): 1896–1898
76. Lou F, Thylen L, Wosinski L. Hybrid plasmonic microdisk resonators for optical interconnect applications. In: Integrated Optics: Physics and Simulations. Prague: Society of Photo-Optical Instrumentation Engineers, 2013
77. Song Y, Wang J, Yan M, Qiu M. Subwavelength hybrid plasmonic nanodisk with high Q factor and Purcell factor. Journal of Optics, 2011, 13(7): 075001-1–075001-5
78. Xu P, Huang Q, Shi Y. Silicon hybrid plasmonic Bragg grating reflectors and high Q-factor micro-cavities. Optics Communications, 2013, 289: 81–84
79. Yang X, Ishikawa A, Yin X, Zhang X. Hybrid photonic-plasmonic crystal nanocavities. ACS Nano, 2011, 5(4): 2831–2838
80. Yu P, Qi B, Xu C, Hu T, Jiang X Q, Wang M H, Yang J Y. An

improved surface-plasmonic nanobeam cavity for higher *Q* and smaller *V*. Chinese Science Bulletin, 2012, 57(25): 3371–3374
81. Alam M, Aitchsion J S, Mojahedi M. Compact hybrid TM-pass polarizer for silicon-on-insulator platform. Applied Optics, 2011, 50(15): 2294–2298
82. Guan X W, Xu P P, Shi Y C, Dai D X. Ultra-compact broadband TM-pass polarizer using a silicon hybrid plasmonic waveguide grating. In: Proceedings of Asia Communications and Photonics Conference. Beijing, 2013, ATh4A
83. Guan X W, Xu P P, Shi Y C, Dai D X. Ultra-compact and ultra-broadband TE-pass polarizer with a silicon hybrid plasmonic waveguide. In: Proceedings of SPIE Photonics West. San Francisco, 2014, 8988
84. Alam M Z, Aitchison J S, Mojahedi M. Compact and silicon-on-insulator-compatible hybrid plasmonic TE-pass polarizer. Optics Letters, 2012, 37(1): 55–57
85. Huang Y, Zhu S, Zhang H, Liow T Y, Lo G Q. CMOS compatible horizontal nanoplasmonic slot waveguides TE-pass polarizer on silicon-on-insulator platform. Optics Express, 2013, 21(10): 12790–12796
86. Sun X, Alam M Z, Wagner S J, Aitchison J S, Mojahedi M. Experimental demonstration of a hybrid plasmonic transverse electric pass polarizer for a silicon-on-insulator platform. Optics Letters, 2012, 37(23): 4814–4816
87. Chee J, Zhu S, Lo G Q. CMOS compatible polarization splitter using hybrid plasmonic waveguide. Optics Express, 2012, 20(23): 25345–25355
88. Gao L F, Hu F F, Wang X J, Tang L X, Zhou Z P. Ultracompact and silicon-on-insulator-compatible polarization splitter based on asymmetric plasmonic-dielectric coupling. Applied Physics. B, Lasers and Optics, 2013, 113(2): 199–203
89. Guan X W, Wu H, Shi Y C, Wosinski L, Dai D X. Ultracompact and broadband polarization beam splitter utilizing the evanescent coupling between a hybrid plasmonic waveguide and a silicon nanowire. Optics Letters, 2013, 38(16): 3005–3008
90. Lou F, Dai D X, Wosinski L. Ultracompact polarization beam splitter based on a dielectric-hybrid plasmonic-dielectric coupler. Optics Letters, 2012, 37(16): 3372–3374
91. Sun B, Chen M Y, Zhang Y K, Zhou J. An ultracompact hybrid plasmonic waveguide polarization beam splitter. Applied Physics B, Lasers and Optics, 2013, 113(2): 179–183
92. Guan X W, Wu H, Shi Y C, Dai D X. Extremely small polarization beam splitter based on a multimode interference coupler with a silicon hybrid plasmonic waveguide. Optics Letters, 2014, 39(2): 259–262
93. Caspers J N, Alam M Z, Mojahedi M. Compact hybrid plasmonic polarization rotator. Optics Letters, 2012, 37(22): 4615–4617
94. Caspers J N, Aitchison J S, Mojahedi M. Experimental demonstration of an integrated hybrid plasmonic polarization rotator. Optics Letters, 2013, 38(20): 4054–4057
95. Gao L, Huo Y, Harris J S, Zhou Z. Ultra-compact and low-loss polarization rotator based on asymmetric hybrid plasmonic waveguide. IEEE Photonics Technology Letters, 2013, 25(21): 2081–2084
96. Song Y, Wang J, Li Q, Yan M, Qiu M. Broadband coupler between silicon waveguide and hybrid plasmonic waveguide. Optics Express, 2010, 18(12): 13173–13179
97. Zhu S, Lo G, Kwong D. Analysis of ultracompact silicon electro-optic modulator based on Cu-insulator-Si hybrid plasmonic donut resonator. In: Proceedings of Photonics Global Conference. Singapore, 2012
98. Ooi K J A, Bai P, Chu H, Ang L K. Vandium dioxide active plasmonics. In: Proceedings of Photonics Global Conference. Singapore, 2012
99. Sun X M, Zhou L J, Li X W, Hong Z H, Liu S, Chen J P. Miniature intensity modulator based on a silicon-polymer hybrid plasmonic waveguide. In: Proceedings of SPIE Photonics and Optoelectronics Meetings. Shanghai, 2011, 8333
100. Lou F, Dai D X, Thylen L, Wosinski L. Design and analysis of ultra-compact EO polymer modulators based on hybrid plasmonic microring resonators. Optics Express, 2013, 21(17): 20041–20051
101. Dalton L R, Robinson B, Jen A, Ried P, Eichinger B, Sullivan P, Akelaitis A, Bale D, Haller M, Luo J, Liu S, Liao Y, Firestone K, Bhatambrekar N, Bhattacharjee S, Sinness J, Hammond S, Buker N, Snoeberger R, Lingwood M, Rommel H, Amend J, Jang S H, Chen A, Steier W. Electro-optic coefficients of 500 pm/V and beyond for organic materials. In: Proceeding of SPIE 5935, Linear and Nonlinear Optics of Organic Materials V. 2005
102. Sun X M, Zhou L J, Li X W, Hong Z H, Chen J P. Design and analysis of a phase modulator based on a metal-polymer-silicon hybrid plasmonic waveguide. Applied Optics, 2011, 50(20): 3428–3434
103. Zhou G, Wang T, Su Y. Broadband optical parametric amplifier in ultra-compact plasmonic waveguide. In: Proceedings of Asia Communications and Photonics Conference. Shanghai, 2010, 79870A
104. Bahrami F, Alam M Z, Aitchison J S, Mojahedi M. Dual polarization measurements in the hybrid plasmonic biosensors. Plasmonics, 2013, 8(2): 465–473
105. Kwon M S. Theoretical investigation of an interferometer-type plasmonic biosensor using a metal-insulator-silicon waveguide. Plasmonics, 2010, 5(4): 347–354
106. Zhou L J, Sun X M, Li X W, Chen J P. Miniature microring resonator sensor based on a hybrid plasmonic waveguide. Sensors (Basel, Switzerland), 2011, 11(7): 6856–6867
107. Zhang L, Shu Y. Modified hybrid plasmonic waveguides as tunable optical tweezers. Chinese Physics Letters, 2013, 30(3): 034208-1–034208-4
108. Yang X, Liu Y, Oulton R F, Yin X, Zhang X. Optical forces in hybrid plasmonic waveguides. Nano Letters, 2011, 11(2): 321–328
109. Guan X, Wu H, Dai D. Silicon hybrid surface plasmonic nano-optics-waveguide and integrated devices. Chinese Journal of Optics and Applied Optics, 2014, 7(2): 181–196
110. Liang D, Fiorentino M, Okumura T, Chang H H, Spencer D T, Kuo Y H, Fang A W, Dai D, Beausoleil R G, Bowers J E. Electrically-pumped compact hybrid silicon microring lasers for optical interconnects. Optics Express, 2009, 17(22): 20355–20364
111. Dong P, Feng N N, Feng D, Qian W, Liang H, Lee D C, Luff B J, Banwell T, Agarwal A, Toliver P, Menendez R, Woodward T K, Asghari M. GHz-bandwidth optical filters based on high-order silicon ring resonators. Optics Express, 2010, 18(23): 23784–23789

112. Xu Q, Schmidt B, Pradhan S, Lipson M. Micrometre-scale silicon electro-optic modulator. Nature, 2005, 435(7040): 325–327
113. Wang J W, Dai D X. Highly sensitive Si nanowire-based optical sensor using a Mach-Zehnder interferometer coupled microring. Optics Letters, 2010, 35(24): 4229–4231
114. Dekker R, Usechak N, Forst M, Driessen A. Ultrafast nonlinear all-optical processes in silicon-on-insulator waveguides. Journal of Physics D, 2007, 40(14): R249–R271
115. Dai D X, Liu L, Gao S M, Xu D X, He S L. Polarization management for silicon photonic integrated circuits. Laser Photonics Review, 2013, 7(3): 303–328
116. Dai D, Tang Y, Bowers J E. Mode conversion in tapered submicron silicon ridge optical waveguides. Optics Express, 2012, 20(12): 13425–13439
117. Wang Z W, Dai D X. Ultrasmall Si-nanowire based polarization rotator. Journal of the Optical Society of America. B, Optical Physics, 2008, 25(5): 747–753
118. Cardenas J, Poitras C B, Robinson J T, Preston K, Chen L, Lipson M. Low loss etchless silicon photonic waveguides. Optics Express, 2009, 17(6): 4752–4757
119. Mote R G, Chu H S, Bai P, Li E P. Compact and efficient coupler to interface hybrid dielectric-loaded plasmonic waveguide with silicon photonic slab waveguide. Optics Communications, 2012, 285(18): 3709–3713
120. Choi S E, Kim J T. Vertical coupling characteristics between hybrid plasmonic slot waveguide and Si waveguide. Optics Communications, 2012, 285(18): 3735–3739
121. Shi P, Zhou G, Chau F S. Enhanced coupling efficiency between dielectric and hybrid plasmonic waveguides. Journal of the Optical Society of America. B, Optical Physics, 2013, 30(6): 1426–1431
122. De Leon I, Berini P. Amplification of long-range surface plasmons by a dipolar gain medium. Nature Photonics, 2010, 4(6): 382–387
123. Noginov M A, Zhu G, Mayy M, Ritzo B A, Noginova N, Podolskiy V A. Stimulated emission of surface plasmon polaritons. Physical Review Letters, 2008, 101(22): 226806
124. Ambati M, Nam S H, Ulin-Avila E, Genov D A, Bartal G, Zhang X. Observation of stimulated emission of surface plasmon polaritons. Nano Letters, 2008, 8(11): 3998–4001
125. van den Hoven G N, Koper R J I M, Polman A, van Dam C, van Uffelen J W M, Smit M K. Net optical gain at 1.53 μm in Er-doped Al_2O_3 waveguides on silicon. Applied Physics Letters, 1996, 68 (14): 1886–1888
126. Grandidier J, des Francs G C, Massenot S, Bouhelier A, Markey L, Weeber J C, Finot C, Dereux A. Gain-assisted propagation in a plasmonic waveguide at telecom wavelength. Nano Letters, 2009, 9(8): 2935–2939
127. Nezhad M, Tetz K, Fainman Y. Gain assisted propagation of surface plasmon polaritons on planar metallic waveguides. Optics Express, 2004, 12(17): 4072–4079
128. Plum E, Fedotov V A, Kuo P, Tsai D P, Zheludev N I. Towards the lasing spaser: controlling metamaterial optical response with semiconductor quantum dots. Optics Express, 2009, 17(10): 8548–8551
129. Bolger P M, Dickson W, Krasavin A V, Liebscher L, Hickey S G, Skryabin D V, Zayats A V. Amplified spontaneous emission of surface plasmon polaritons and limitations on the increase of their propagation length. Optics Letters, 2010, 35(8): 1197–1199
130. Seidel J, Grafström S, Eng L. Stimulated emission of surface plasmons at the interface between a silver film and an optically pumped dye solution. Physical Review Letters, 2005, 94(17): 177401
131. Radko I, Nielsen M G, Albrektsen O, Bozhevolnyi S I. Stimulated emission of surface plasmon polaritons by lead-sulphide quantum dots at near infra-red wavelengths. Optics Express, 2010, 18(18): 18633–18641
132. Pavesi L, Dal Negro L, Mazzoleni C, Franzò G, Priolo F. Optical gain in silicon nanocrystals. Nature, 2000, 408(6811): 440–444
133. Gather M C, Meerholz K, Danz N, Leosson K. Net optical gain in a plasmonic waveguide embedded in a fluorescent polymer. Nature Photonics, 2010, 4(7): 457–461
134. Rao R J, Tang T T. Study of an active hybrid gap surface plasmon polariton waveguide with nanoscale confinement size and low compensation gain. Journal of Physics. D, Applied Physics, 2012, 45(24): 245101
135. Zhang J, Cai L, Bai W L, Xu Y, Song G F. Hybrid plasmonic waveguide with gain medium for lossless propagation with nanoscale confinement. Optics Letters, 2011, 36(12): 2312–2314
136. Zhu N, Mei T. Study of an SPP mode with gain medium based on a hybrid plasmonic structure. In: Proceedings of Asia Communications and Photonics Conference (ACP). Guangzhou, 2012, AF4A.17
137. Gao L F, Tang L X, Hu F F, Guo R M, Wang X J, Zhou Z P. Active metal strip hybrid plasmonic waveguide with low critical material gain. Optics Express, 2012, 20(10): 11487–11495
138. Ma R M, Oulton R F, Sorger V J, Bartal G, Zhang X. Room-temperature sub-diffraction-limited plasmon laser by total internal reflection. Nature Materials, 2011, 10(2): 110–113
139. Zhu S, Lo G Q, Kwong D L. Theoretical investigation of ultracompact and athermal Si electro-optic modulator based on Cu-TiO_2-Si hybrid plasmonic donut resonator. Optics Express, 2013, 21(10): 12699–12712
140. Zhou G, Wang T, Su Y. Broadband optical parametric amplifier in ultra-compact plasmonic waveguide. In: Proceedings of Asia Communications and Photonics Conference. Shanghai, 2010, 79870A
141. Zhang J, Cassan E, Zhang X. Efficient second harmonic generation from mid-infrared to near-infrared regions in silicon-organic hybrid plasmonic waveguides with small fabrication-error sensitivity and a large bandwidth. Optics Letters, 2013, 38(12): 2089–2091
142. Aldawsari S, West B R. Hybrid plasmonic waveguides for nonlinear applications. In: Proceedings of Photonics Global Conference. Singapore, 2012
143. Pitilakis A, Kriezis E E. Highly nonlinear hybrid silicon-plasmonic waveguides: analysis and optimization. Journal of the Optical Society of America. B, Optical Physics, 2013, 30(7): 1954–1965
144. Perron D, Wu M, Horvath C, Bachman D, Van V. All-plasmonic switching based on thermal nonlinearity in a polymer plasmonic microring resonator. Optics Letters, 2011, 36(14): 2731–2733
145. Lu C C, Hu X Y, Yue S, Fu Y L, Yang H, Gong Q H. Ferroelectric hybrid plasmonic waveguide for all-optical logic gate applications. Plasmonics, 2013, 8(2): 749–754

146. Li F, Xu M, Hu X F, Wu J Y, Wang T, Su Y K. Monolithic silicon-based 16-QAM modulator using two plasmonic phase shifters. Optics Communications, 2013, 286: 166–170
147. Luo Y, Chamanzar M, Eftekhar A A, Adibi A. Dual structures for ultra-compact on-chip plasmonic light concentration on silicon platforms. In: Proceedings of IEEE Photonics Conference, Burlingame, 2012, 682–683
148. Zhu N, Mei T. Focusing and demultiplexing of an in-plane hybrid plasmonic mode based on the planar concave grating. Optics Communications, 2013, 298-299: 120–124
149. Ketzaki D A, Tsilipakos O, Yioultsis T V, Kriezis E E. Electromagnetically induced transparency with hybrid silicon-plasmonic traveling-wave resonators. Journal of Applied Physics, 2013, 114(11): 11317-1–11317-8
150. Zhu N, Mei T. Analysis of an ultra-compact wavelength filter based on hybrid plasmonic waveguide structure. Optics Letters, 2012, 37(10): 1751–1753
151. Akimov Y A, Chu H S. Plasmon-plasmon interaction: controlling light at nanoscale. Nanotechnology, 2012, 23(44): 444004
152. Hu Y W, Li B B, Liu Y X, Xiao Y F, Gong Q. Hybrid photonic-plasmonic mode for refractometer and nanoparticle trapping. Optics Communications, 2013, 291: 380–385
153. Lanzillotti-Kimura N D, Zentgraf T, Zhang X. Control of plasmon dynamics in coupled plasmonic hybrid mode microcavities. Physical Review B: Condensed Matter and Materials Physics, 2012, 86(4): 045309-1–045309-6
154. Zhang T, Chen L, Li X. Reduction of propagation loss by introducing hybrid plasmonic model in graded-grating based “trapped rainbow” system. Optics Communications, 2013, 301-302: 116–120
155. Zhu S, Lo G Q, Kwong D L. Theoretical investigation of silicide Schottky barrier detector integrated in horizontal metal-insulator-silicon-insulator-metal nanoplasmonic slot waveguide. Optics Express, 2011, 19(17): 15843–15854
156. He X Y, Wang Q J, Yu S F. Numerical study of gain-assisted terahertz hybrid plasmonic waveguide. Plasmonics, 2012, 7(3): 571–577

Xiaowei Guan received the B.Eng. degree from the Department of Electronic Science and Engineering, Southeast University, Nanjing, China, in 2009. He is currently working toward the Ph.D. degree in the Department of Optical Engineering, Zhejiang University, Hangzhou, China. His research interests include the design and fabrication of silicon-based nanophotonic/nanoplasmonic waveguides and devices.

Hao Wu received the B.Eng. degree from the Department of Optical Engineering, Zhejiang University, Hangzhou, China, in 2013. He is currently working toward the Ph.D. degree in the same department of Zhejiang University. His research interests include silicon nanophotonic integrated waveguides and the applications.

Daoxin Dai received the B. Eng. degree from Department of Optical Engineering, Zhejiang University (China), and the Ph.D. degree from Royal Institute of Technology (Sweden), in 2000 and 2005, respectively. He joined Zhejiang University as an assistant professor in 2005 and became an associate professor in 2007, a full professor in 2011. He visited the Chinese University of Hong Kong in 2005, and Inha University (Korea) in 2007. Dr. Dai worked at the University of California, Santa Barbara as a visiting scholar from the end of 2008 until 2011. His current research interests include silicon nanophotonics for optical interconnections and optical sensing. He has published about 110 refereed international journals papers (including 6 invited review papers), and holds 9 patents. Dr. Dai has been invited to give more than 10 invited talks and served as the program committee member or session chair for some top international conferences. He is serving as the Associate Editor of the Journals of “Optical and Quantum Electronics” and “Photonics Research”.